Quality Assurance of Lung Cancer CT Screening CAD Systems: Feasibility Study with PSF-based Virtual Nodules

Janaka C Marasinghe

February 2015

Graduate School of Health Sciences

Niigata University, Japan.

Quality Assurance of Lung Cancer CT Screening CAD Systems: Feasibility Study with PSF-based Virtual Nodules

Janaka C Marasinghe

Graduate School of Health Sciences, Niigata University, Japan.

Supervisor: Prof. Shinichi Wada.

Abstract

Computer-aided detection/diagnosis (CAD) is increasingly used in clinical practice. CAD systems are useful for decision making in detection and interpretation of diseases by clinicians. Therefore, quality assurance (QA) for CAD has a key role in clinics and it helps end users to make aware of changes in CAD performance both due to intentional or unintentional causes. However, there are no QA requirements for CAD in clinical use at present. CAD subcommittee of American Association of Physicists in Medicine (AAPM) has recently published the general guidelines for all CAD systems used in clinical practice. Further to that need of research studies to find appropriate methods for QA of CAD systems has been pointed out by the publication.

Purpose of my study is to introduce a new method to assess lung cancer CT screening CAD systems' performance effectively and perform QA of the same CAD system.

First part of the study was performed to verify the point spread function (PSF)-based virtual nodules. 19 clinical lung nodules of 18 subjects were used from screening data set of a general hospital for the verification study. These nodules were confirmed by experienced lung screening radiologist. PSF-based nodules were simulated with quite similar size and density of each clinical nodule. Then superimposed on same images and CAD were performed. Similar free response receiver characteristic (FROC) curves were obtained for both clinical lung nodules and comparable PSF-based virtual nodules. This result implies that the CAD system

has shown a similar performance on both clinical nodules and PSF-based virtual nodules. Therefore, this result verifies the PSF-based virtual nodules.

Then the feasibility of PSF-based virtual nodules was checked for assessing CAD system performance in detail. PSF-based nodules were simulated with various sizes and densities and superimposed on clinical images to assess the CAD performance dependence on nodule size and density and slice thickness. FROC curves are used to analyze results. Nodule size study shows true positive fraction (TPF) is higher for larger nodules. Nodule density study shows that TPF is larger for higher density nodules. Slice thickness study shows that higher percentages of nodules on thick slices were detected by the tested CAD system. Therefore, tested lung cancer CT screening CAD system shows tendency of performance on high dense large nodules on thick slices.

Similarly the proposed PSF-based virtual nodules can be used to assess the performance of a CAD system with images from various clinics with different scan/reconstruction conditions. PSF-based virtual nodule method applies its own images of a clinic which includes same scan/reconstruction parameters and avoids the CAD performance dependence on special resolution conditions. Therefore, this method is feasible to apply for QA of lung cancer CT screening CAD systems at any different clinical sited for different CAD systems.

Study results show that practical implementation of QA for CAD system is possible with the proposed method. Therefore, this study proposed PSF-based virtual nodules based QA protocol for lung cancer CT screening CAD system.

Contents

Page no.

Abstract i

List of Figures v

List of Tables vi

Chapter 1 Introduction 1

1. 1. Lung cancer CT screening 1

1. 2. CAD systems 5

1. 3. QA for clinical lung cancer CT screening CAD systems. 8

1.3.1. When does a QA procedure need to be performed? 10

1.3.2. What are the tools and materials that may be used to perform the QA tests? 11

1.3.3. What are the performance measures to be used? 12

Chapter 2 Theory of generating PSF-based virtual nodules 15

2. 1. Principle of computer simulation 15

2. 2. 3D PSF measurements 17

Chapter 3 Verification of PSF-based virtual nodules by lung CAD using CT screening database 19

3. 1. Introduction 19

3. 2. Materials and Methods 21

3. 3. Results 29

3. 4. Discussion 32

Chapter 4 CAD performance with different conditions 33

4.1. CAD of different nodule sizes 33

4.1.1. Introduction 33

4.1.2. Materials and Methods 34

4.1.3. Results 36

4.1.4. Discussion 39

4.2. CAD of different nodule densities 40

4.2.1. Introduction 40

4.2.2. Materials and Methods 40

4.2.3. Results 41

4.2.4. Discussion 44

4.3. CAD performance with thin and thick slices 45

4.3.1. Introduction 45

4.3.2. Materials and Methods 45

4.3.3. Results 46

4.3.4. Discussion 48

Chapter 5 Discussion 50

Chapter 6 Conclusion 56

Reference list 57

Acknowledgement 67

List of Figures

Page no.

Figure 2-1 Generation of computer-simulated nodule in scan (xy) plane. 15

Figure 2-2 Generation of computer-simulated nodule in zx plane 16

Figure 2-3 Phantom used for the PSF measurements 17

Figure 3-1 Flowchart of the nodule size measurement 22

Figure 3-2 Calibration curve for nodule size 23

Figure 3-3 Estimation of real nodule size 24

Figure 3-4 Flowchart of the nodule density measurement 25

Figure 3-5 Calibration curve for nodule density 26

Figure 3-6 Generation of virtual nodules 27

Figure 3-7 Selected three cases for real nodule and superimposed simulated nodules 28

Figure 3-8 Sample detections by the CAD system 29

Figure 3-9 FROC curves for real nodules and PSF-based virtual nodules 31

Figure 4-1 Virtual nodule images fused on three locations of the lung field 35

Figure 4-2 CAD detections of virtual nodules having different sizes and same density 36

Figure 4-3 FROC curves for different nodule sizes 37

Figure 4-4 CAD detections of virtual nodules having different densities 41

Figure 4-5 FROC curves for different nodule densities 43

Figure 4-6 Sample nodule detection by CAD system on thin slices 47

Figure 4-7 Sample nodule detection by CAD system on thick slices 47

Figure 4-8 FROC curves for thin and thick slices 49

Figure 5-1 Flow of the QA protocol 52

List of Tables

Page no.

Table 1-1 Five-year survival rate for all patients with lung cancer diagnosis 2

Table 3-1 Measurement details of nodule size and density 30

Table 4-1 p-Values for each pair of different nodule sizes 38

Table 4-2 p-Values for each pair of different nodule densities 42

Chapter 1 Introduction

1. 1. Lung cancer CT screening

1.1.1

Lung cancer is the leading cause of cancer-related deaths in the world and it is the number one cause of cancer-related deaths in males and the second leading cause of cancer-related deaths in females [1]. Approximately 95% of those diagnosed with lung cancer die from it [2]. Symptoms of lung cancer generally produce in the well advanced stages of the diseases. More than 10% of diagnoses are made incidentally following a chest radiograph for an unrelated reason. Therefore effective treatment options are limited and prognosis is poor due to the advance stage of the lung cancer [3]. The 5-year survival rate for lung cancer varies by country but is generally 5–15% [1, 4]. Findings from the early lung cancer action project (ELCAP) conforms that survival rates are highest for those whose cancer is detected early stages (Table 1-1). ELCAP has suggested a 10-year survival rate of 88% for patients with stage I lung cancers. Further, ELCAP has suggested that low-dose computed tomography (LDCT) screening can be prevented 80% of deaths from lung cancer in high-risk groups [2].

1.1.2 Basic principle of screening

There are number of basic principles established for lung cancer CT screening programs.

- First, the screening test must not cause harm. LDCT is a non-contrast study conducted during a single breath hold lasting approximately15-20 seconds [5].

- Second, the screening test must be highly accurate at detecting treatable, preclinical disease. Analysis of initial screening results during one randomized trial indicated a sensitivity of 94.6% with a positive predictive value of 35.7% [6].
- Third, the screening population must have a high prevalence of detectable preclinical disease. The specificity of a screening program depends on the prevalence of the disease. Smoking is the most important risk factor for lung cancer. 85% of lung cancer-related deaths are associate with smoking and higher relative risk of developing lung cancer.

Table 1-1. Five-year survival rate for all patients with lung cancer diagnosis

Stage	5-year survival rate (%)
IA	49
IB	45
IIA	30
IIB	31
IIIA	14
IIIB	5
IV	1

1.1.3 Lung cancer screening trials

Number of lung cancer screening trials has conducted in fast. Radiographs were used in 1960s and 1970s. However, due to the lower resolution of radiographs those

studies were not concluded [7,8]. The advent of CT allowed considerable improvement of sensitivity, and several studies have been conducted using LDCT as the screening tool. In 1990s group of Japanese investigators [9,10] initiated the screening for lung cancers by using CT. They demonstrated that LDCT is feasible to detect about 3 times more lung cancers than chest radiography [11, 12]. Following that number of normalized and randomized trials has been conducted. Results of some major programs such as ELCAP and National Lung Screening Trial (NLST) have been published and the results of Dutch-Belgian randomized lung cancer multislice CT screening (NELSON) trial are expected in 2015. NLST was the first prospective randomized trial comparing screening efficacy of LDCT and chest radiograph using mortality as an end point. Results show that LDCT screening can reduce the mortality from lung cancer 20% more than by screening with chest radiographs. This study concludes that LDCT screening can reduce the mortality [7].

Overall goal of the LDCT screening is to reduce mortality from lung cancer. Studies have shown the benefits of the LDCT screening. One important benefit is early diagnosis of lung cancer which help to reduce the risk of mortality because early stage lung cancer potentially curable and needs only less invasive surgical techniques [13]. Another indirect benefit of screening program is increasing the number of participants for smoking cessation programs [14, 15].

However, mass screening based on helical CT images leads to a considerable number of images to be evaluated; this is time-consuming and makes its use difficult in the clinic [16]. Therefore, computer aided detection/diagnosis (CAD) system for

lung cancer screening is a feasible solution to decrease the work load of clinicians and increases the nodule detection efficiency [17 - 20].

1. 2. CAD systems

Medical imaging has been indispensable in medicine since the discovery of x-rays. Medical imaging offers useful information on patients' medical conditions and on the causes of their symptoms and diseases. With the advancement of imaging technologies, a large number of medical images are produced which the radiologist has to analyze and evaluate comprehensively in a short time. It has long been recognized that clinicians do not always make optimal use of the data acquired by an imaging device [21, 22]. The limitations of the human eye-brain system, limitations in training and experience, and factors such as fatigue, distraction, and satisfaction of search may all contribute to suboptimal use of available information [23 - 25]. Medical image processing attempts to modify the image presented to the readers in such a manner that abnormalities are enhanced for the human visual system. However, image processing alone is unlikely to completely address factors such as fatigue, distraction, or limitations in training. CAD systems applied to medical images go beyond image processing, such that they may provide specific lesion location information and/or other diagnostic analysis to assist clinicians [26]. Therefore, computer aids are demanded and become indispensable in physicians' decision making based on medical images. Consequently, computer-aided detection and diagnosis has been investigated and has been an active research area in medical imaging. [27 - 31]. Basically computer aid is used for two major tasks of computer aided detection and computer aided diagnosis. CAD systems mark regions of an image that may reveal specific abnormalities and are used to alert clinicians to these regions during image interpretation. Computer-aided diagnosis systems provide an

assessment of a disease using image-based information alone or in combination with other relevant diagnostic data and are used by clinicians as a decision support in developing their diagnoses. The first study of applying computer aids in radiology was published by Winsberg et al. in 1967 [32]. This study conducted to detect abnormalities in mammograms. After that computer aided detections have studied to apply in various areas such as detecting focal abnormalities in chest radiographs, heart abnormalities, angiography, detection of lung nodules in chest radiography, detection of interstitial lung diseases in chest radiography, lung nodule detection in chest CT, breast magnetic resonance imaging (MRI), breast ultrasound and detection of polyps in CT colonography. The success of a particular CAD system can be measured in terms of accuracy of diagnosis, speed, and automation level. In 1988, U.S. Food and drug Administration has approved the first commercial CAD system which was developed by researchers from University of Chicago for mammograms and the system has commercialized by R2 Technology Inc. Following that CAD systems are commercially available for other imaging modalities too [33].

Early detection of the small lung nodule is the target of lung screening. CAD system can play a key role in lung cancer CT screening and help to reduce the mortality. Research results show that the combination of a radiologist and CAD as a second reader can significantly improve the detection rates of lung nodules, and it has been recommended and proposed to use a CAD system for daily routine work [17 - 20, 34]. Consequently, CAD system for lung cancer CT screening has become an attractive research interest in medical imaging and diagnostic radiology. Many studies of performance evaluations of CAD systems have been carried out using clinical

image databases [17 - 20, 35 - 43]. As the image databases included actual nodules with complicated shapes and heterogeneous density, the CAD performance evaluated with using the database was considered as an overall performance for various size and density of nodules, not for specific nodule characteristics. Although the CAD systems for lung cancer CT screening are commercially available, standardized approaches for evaluating and reporting their performance have not yet been fully formalized in the literature or in a standardization effort and research on quality assurance (QA) of CAD is limited to date [44]. In my study I have focused on this matter and proposed a QA protocol for CAD system for lung cancer CT screening by applying point spread function (PSF)-based virtual nodules.

1. 3. QA for clinical lung cancer CT screening CAD system

CAD is increasingly used in clinical practice. CAD systems are useful for decision making in detection and interpretation of diseases by clinicians. Therefore, quality assurance (QA) for CAD has a key role in clinics and it helps end users to make aware of changes in CAD performance both due to intentional or unintentional causes. However, there are no QA requirements for CAD in clinical use at present. Need of QA for CAD systems has identified and published by CAD subcommittee of American association of physicists in medicine (AAPM) as recommended general QA guidelines common for all CAD systems. This lack of QA has led to difficulty in the comparison of available CAD system and to understand the CAD performance variation under different clinical practices [26].

Basically the clinical applications of products are done considering the risk-benefit profile associate with them. CAD performance may change with the time and therefore the initial risk-benefit profiles also change. Thus, QA testing throughout the life cycle of CAD is essential to assure the consistency of CAD system performance over time. Without having a routine QA practice, clinicians may not be alerted to any unexpected changes in CAD performance and do not have the ability to easily identify any potential issue that may arise. Therefore, acceptance test should be performed ensuring the CAD system functions correctly when installed at clinic and conform the specifications given by the manufacturer. Routinely check of CAD performance is needed to identify weather the initial performance has changed significantly. CAD systems used in different clinical applications should apply a feasible QA protocols depending on its application.

In this study I introduced a newly developed feasible method of QA for lung cancer CT screening CAD system following recommended general QA guidelines published by AAPM [44]. These general guidelines are based on 7 matters.

Q1. When does a QA procedure need to be performed?

Q2. Who should perform the test?

Q3. What are the tools and materials that may be used to perform the QA tests?

Q4. What are the performance measures to be used?

Q5. What QA results should be captured and how should they be reported?

Q6. What are the criteria of success/failure of the tests (or minimal requirements)?

Q7. What should be done if the CAD QA test fails?

Depending on the particular CAD application responds to these questions are varied. In my study I mainly focused on the lung cancer CT screening CAD systems and tried to find the responses mainly for the points raised in Q1, Q3 and Q4.

1.3.1. When does a QA procedure need to be performed?

Selection of an appropriate lung cancer CT screening CAD system for a particular screening clinic is one of the critical issues to be considered. This selection should be done carefully considering many factors as explained in the discussion section. Once an appropriate CAD system has been selected and installed, it is the hospital staff's (e.g., diagnostic medical physicist, radiologist and radiological technologist) responsibility to assure that the equipment functions correctly, according to all published claims made by the CAD developer. This is the time to do performance verification and conformation of the specification documented and created during the selection process. This process is called the acceptance testing [45]. Documentation of the system performance during the warranty period may become a critical issue and hence must be carefully maintained. Following successful installation and acceptance, CAD system must be monitored on an ongoing basis to ensure continued, reliable performance. This routine QA practice with a periodic evaluation procedure is an essential part of QA and the purpose of routine QA testing is to identify any changes of CAD performance that may result in a clinically significant degradation. One of the other critical situations when the CAD QA tests are recommended is after upgrading or changing the CT scanner's software or CAD system's software. Further to that replacement of CT scanners hardware components which affect image quality also leads to a CAD performance variation, hence the QA tests are recommended after such replacement. Main hardware changes are X-ray tube or detector system and the main software change that effect on image quality is the image reconstruction algorithm. After having any of these changes performance of the lung cancer CT

screening CAD system should be checked and compared with the initial performance. Addition to the situations as discussed earlier, CAD performance may vary due to the change in one or more of image acquisition parameters such as kV, mAs or slice thickness. After such change of image acquisition parameters QA tests are recommended to apply.

1.3.2. What are the tools and materials that may be used to perform the QA tests?

QA for CAD system need to use method which apply feasible materials and tools. These are three proposed materials and tools as follows:

a. Validated software tools provided by the CAD manufacturer or a third party

b. Set of clinical images with appropriate known reference standards provided by the CAD manufacturer or collected at the clinical site and

c. Phantoms that are validated for a specific CAD QA purpose with a validated test procedure.

According to the available literature none of these materials or tools has implemented in the clinical practice of QA yet. Therefore, the most suitable materials or tools should be introduce and validate for the routine clinical use. When the most suitable material or tool is selecting, there are several factors to be considered. It should be cost effective and appropriate to measure the relevant parameter and what QA of lung cancer CT screening CAD system would be performed. If a software tool is selected as a QA tool it should allow user to save and retrieve user-selected image

data for QA and store and analyze results of QA test without interfering with the local patient data. Other proposed option is to use a set of clinical images. In this method numerous nodules in a large-scale image database are necessary to perform a detailed QA test such as effect of CAD on lung nodule characteristics and image acquisition conditions. Collection of a set of clinical images with an appropriate scan/reconstruction condition is a very much time consuming work to an individual clinic. CAD performance evaluation should be performed by using images with the same scan/reconstruction parameters as screenings are done in the clinic where the CAD system is used. Because, CAD performance varies with image quality and therefore it depends on scan/reconstruction parameters. Use of phantom images is worth of consideration as potential resource for lung CAD QA procedures. It would be a solution instead of collecting larger number of screening images from an individual clinic. One important thing is to verify that CAD system performance is relatively close to its response to real clinical images. One major limitation of the physical phantoms is the cost to build a large set of different physical phantoms that will realistically cover the variations in the lesion characteristics and anatomical structures in the patient population.

1.3.3. What are the performance measures to be used?

There are number of measures to be considered in QA for lung cancer CT screening CAD system. Performance measured to be performed depends on the purpose of the QA test. True positive fraction (sensitivity) which is the ratio of detected nodules to the total number of nodules considered is the most commonly used term to evaluate and present the CAD performance. Detection sensitivity depends on number of

factors. One of them is lung nodule characteristics such as its size and density. Therefore, QA test should be performed by applying nodules with known sizes and densities and also the results should be reported accordingly. Image acquisition parameters also affect on the detection sensitivity of lung cancer CT screening CAD system. Therefor image acquisition conditions such as slice thickness, mA, kV and reconstruction kernel should be reported and the changing of sensitivity under these conditions also should be measured.

In my study, I considered the proposed materials and tools and performance measures to be used for QA of CAD under the general guidelines for QA of CAD published by CAD subcommittee of AAPM. I propose a new approach for QA of lung cancer CT screening CAD system based on the PSF measured in the CT system. Partially digital phantom which is a newly proposed concept is the base of this method. Partially digital phantoms are form by superimposing simulated nodules on clinical images [44]. This method can be considered as a combination of all three proposed materials and tools for QA of CAD. Computational tool (software) is used to obtain simulated nodules based on measured PSF of the CT scanner. Then images obtained from the same clinic are used and the simulated nodules are superimposed on those images. Therefore, this partially digital phantom realistically represents the anatomical variation in real lung screening subjects and the same spatial resolution conditions of the clinic. Nodules can be simulated with various sizes, densities and shapes covering clinically diagnosed range and any location from the whole lung field can be selected by considering the probability of detected nodules. Therefore, this independent testing provides a higher level of QA to monitor CAD system

performance in the local patient population and also improve the effectiveness of end users' use of CAD by increasing their understanding of CAD performance in local population. Receiver operating characteristic (ROC) methodology is a widely used method for comparing the performances of imaging modalities. When the number of lesions is more than one, free-response receiver operating characteristic (FROC) is appropriate. Proposed QA method applies more than one virtual nodule on selected subjects' images and therefore, FROC curves are used to compare the CAD performance in QA tests.

Chapter 2 Theory of generating PSF-based virtual nodules

2.1. Principle of computer simulation

Blurring of the CT image can be described by the PSF of a system [46, 47]. The PSF is assumed separable into a two-dimensional (2D) PSF in the x-y scan plane and the SSP in the z-direction perpendicular to the scan plane [48 - 51]. Then, the three dimensional (3D) CT image I (x, y, z) can be expressed as [47, 48, 50]

$$I(x,y,z) = [O(x,y,z) ** PSF(x,y)] * SSP(z), \quad (1)$$

where O(x, y, z) is the object function, PSF(x, y) and SSP(z) are the 2D PSF and slice sensitivity profile, respectively; and ** and * are 2D and 1D convolutions, respectively. Noise and artifact components are neglected in this representation. Figure 2-1 and Figure 2-2 illustrate the generation of 3D image of computer-simulated nodule.

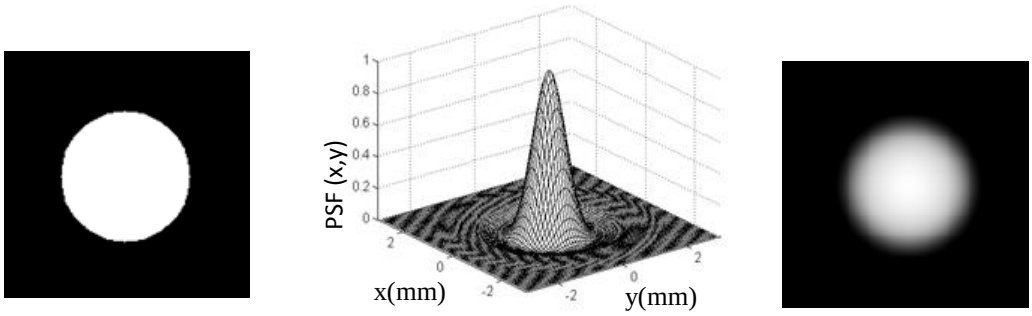

(a) (b) (c)

Figure 2-1. Generation of computer-simulated nodule in scan (xy) plane. (a) Image of the object function in scan plane. (b) 2D PSF in scan plane obtained for reconstruction kernel FC50. (c) Image of the computer-simulated nodule in scan plane

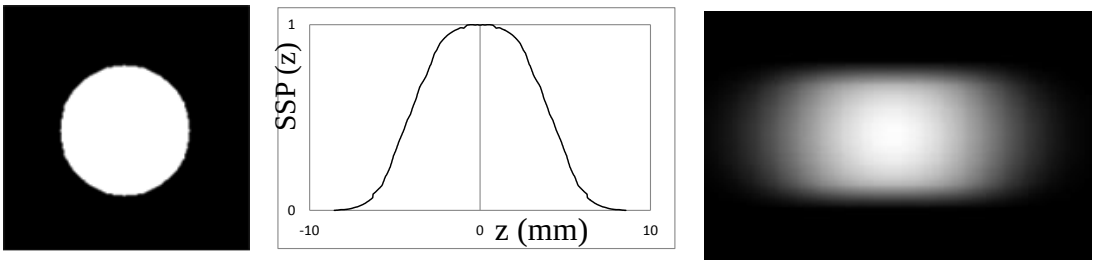

(a) (b) (c)

Figure 2-2. Generation of computer-simulated nodule in perpendicular direction of scan plane (z direction). (a) image of the object function in zx plane. (b) SSP obtained for slice thickness 8 mm. (c) Image of the computer-simulated nodule in zx plane.

2.2. 3D PSF measurements

One important thing of the proposed QA procedure is application of spatial resolution condition of the same scanner at the screening clinic. Therefore, measurement of 2D PSF and the SSP is needed and measured data is used in simulation process. Setting the reconstruction kernel as similar to the screening settings (e.g. FC50 Asteion, Toshiba Medical Systems), 2D PSF measurement of the scanner was performed using a method that determined the 2D PSF in the scan plane by one scan of a commercial phantom, accompanied by verification [49,50]. Figure 2-3 shows an image and a CT scanned image of the phantom used for PSF measurements. This cylindrical phantom

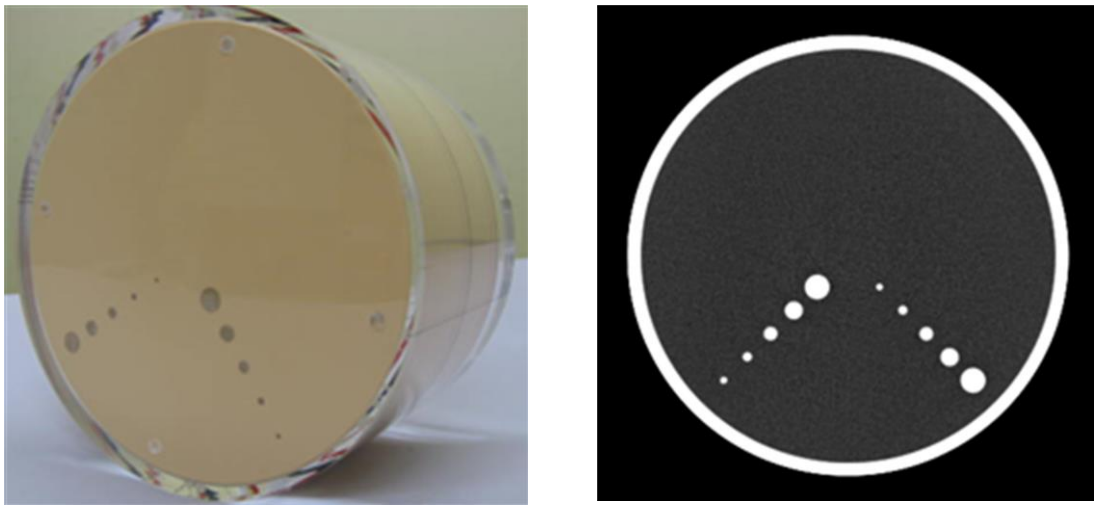

(a) (b)

Figure 2-3. Phantom used for the PSF measurements. (a) Image of the phantom (b) CT scanned image of the phantom.

is filled with the lung tissue equivalent material and contains soft tissue equivalent 10 cylinders placed parallel to the main axis (z-direction). Diameters of the soft tissue equivalent cylinders are 2, 3, 5, 7 and 10 mm. The CT image I(x, y) of such an objects is characterized by its spatial resolution in the scan (xy) plane and does not

depend on the spatial resolution in the z direction, as shown in the following expression:

$$I(x,y) = O(x,y) ** PSF(x,y), \qquad (2)$$

where O(x,y) and PSF(x,y) are two dimensional (2D) object function and the PSF in scan plane respectively. ** represents the 2D convolution. Using the convolution theorem Equation (2) can be transferred as

$$PSF(x,y) = F^{-1}\{F[I(x,y)] / F[O(x,y)]\} \qquad (3)$$

where F and F^{-1} denotes the 2D Fourier transform and the 2D inverse Fourier transform, respectively. The calculation in Equation (3) corresponds to the 2D deconvolution. Phantom was scanned and the CT images of phantom structures were obtained. Then corresponding object [O(x,y)] functions were numerically generated. Then PSF was obtained from Equation (3) [50]. Then setting the slice thickness similar to screening settings (e.g. 8.0 mm), SSP measurement was performed using a commercial phantom (Gold Disk Delta phantom Kyoto Kagaku Co., Ltd., Kyoto, Japan) consisting of a 50-μm-thick gold disk of 1 mm in diameter placed in acrylic.

Chapter 3 Verification of PSF-based virtual nodules by lung CAD using CT screening database

3. 1. Introduction

Application of CAD as a second reader is a well-established technique for increasing the identification of small pulmonary nodules by radiologists on chest CT and has shown good sensitivity for detecting small lung cancers [52]. Therefore, use of CAD systems in clinical practice is increasing rapidly. There should be a QA procedure to check the performance of CAD system from its acceptance test at first installation and consistency of performance over time. For that fixed set of test cases are recommended [44]. This set of cases should represent the patient population as well as the similar spatial resolution conditions used in the same screening clinic. Collection of such test cases as a reference standard required additional effort and experience to estimate the characteristics of nodule on clinical images. Further, it takes considerably long time for an individual clinic collect such set of images and this is not feasible to a new clinic at the starting point. Considering these practical issues my study proposed to apply set of PSF-based virtual nodules having known sizes and densities for QA procedure as a reference standard. Then it is very important to verify that CAD system for lung cancer CT screening response to proposed PSF-based virtual nodules is similar to the its response to real nodules. Purpose of this part of the study is to verify the CAD detection of real nodules and the proposed PSF-based virtual nodules are comparable. Radiologist conformed set of real nodules were chosen from a screening clinic and the similar PSF-based nodules

were generated based on the sizes and densities of each real nodule. Then simulated images were superimposed on corresponding images. Finally the CAD detections were performed and the results were compared by using separate FROC curves for real nodules and virtual nodules.

3. 2. Materials and Methods

Lung cancer CT screening dataset of General Hospital at Nagano, Japan was used with the approval of the institutional review board. In this clinic, applicants have been subjected to lung screening examinations with a multidetector-row CT scanner without contrast enhancement (Asteion, Toshiba Medical Systems, Tokyo, Japan). The imaging parameters were as follows: reconstruction kernel FC50, 120 kV, 30 mA tube current, 8.0 mm slice thickness, 4 detector rows, 0.75 s rotation time and a pitch factor of 1.375. There were 60 total cases in the hospital dataset on which radiologist has detected nodules. Among them, 18 cases (having total of 19 nodules) were selected for the verification study. Selection criteria were such that the nodules have both spherical or elliptical shape and limited to single slice. Therefore, the nodule sizes were limited to about the slice thickness 8 mm.

I applied PSF-based image simulation to simulate lung nodule images. This needs to apply the nodule size to the object function as shown in the Equation (1). Due to the blurring of images, sharp edges of nodules are not visible on clinical CT images and therefore, the true sizes cannot be directly obtained. Apparent size of a nodule is defined as the size appears in the image. The apparent size in the image is apart from its true size. Flowchart (Figure 3-1) shows the steps of obtaining the true nodule size from clinical CT images. Ohkubo et. al. 2008 [53] has published the relationship between the apparent size and true size of simulated images. Based on that publication the relationship between the true size and the apparent size on image of an object was obtained by simulating nodules applying 3 to 10 mm diameters. Measured PSF and SSP values of the same clinic were applied for the simulation

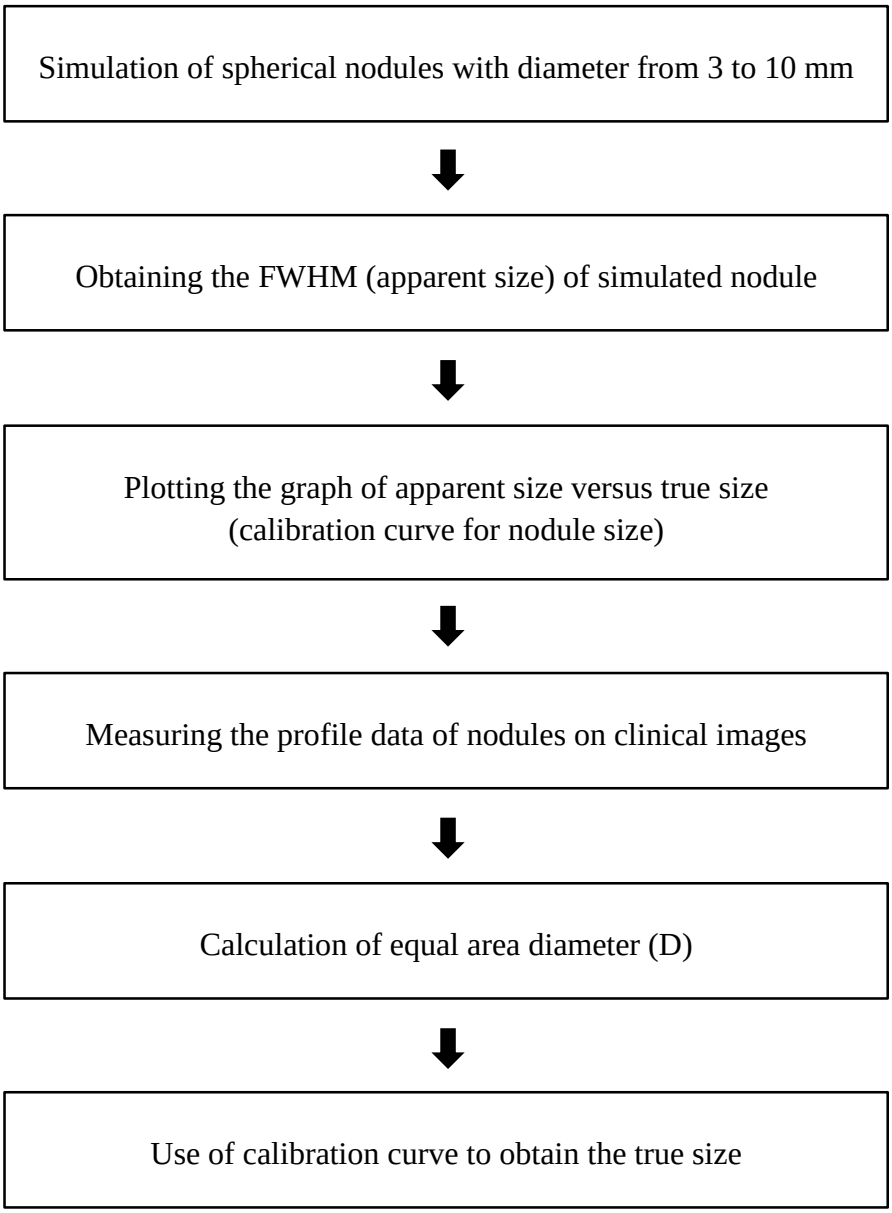

Figure 3-1. Flowchart of the nodule size measurement

process [(Equation (1)]. Full width of half maximum (FWHM) of simulated images has considered as the apparent size of the object on image. Then the apparent sizes for each object function sizes from 3 to 10 mm were obtained by simulating images.

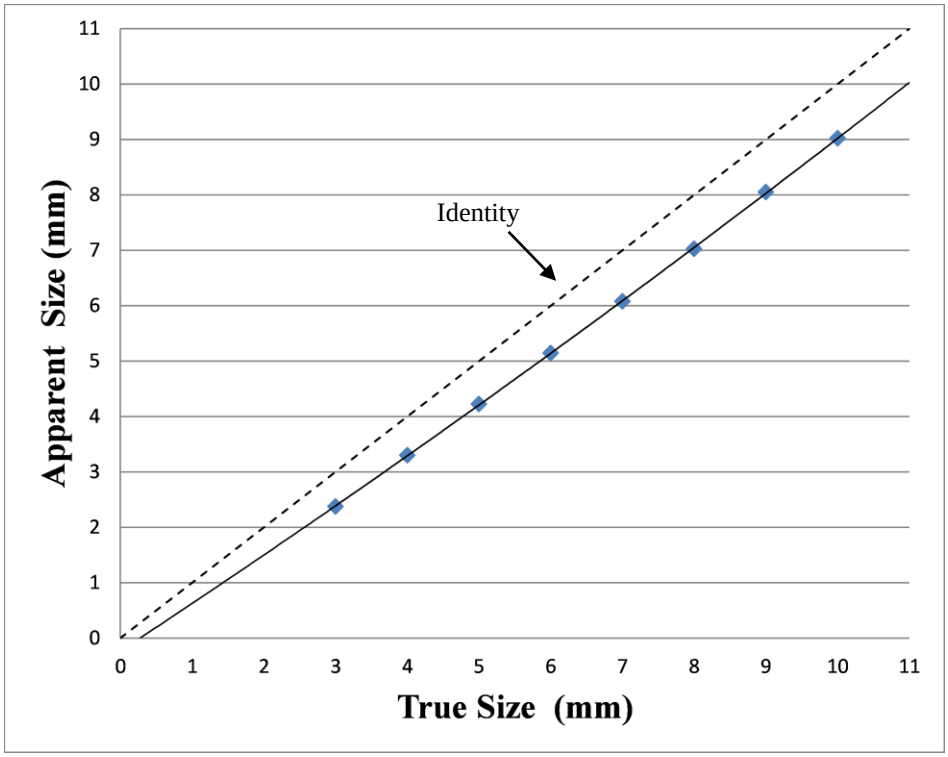

Figure 3-2. Calibration curve for nodule size

After that the graph of apparent size versus true size was obtained (Figure 3-2). If the apparent size of an object on image is known then the corresponding true size can be obtained from this graph. Therefore, this graph can be considered as the calibration curve for nodule size. Next step is to measure the apparent size of selected real nodules on clinical images. Profile data across nodules were used to measure the apparent sizes of nodules. Same conditions were applied for the real nodules also (Figure 3-3).

$$A = \pi \left(\frac{x}{2}\right)\left(\frac{y}{2}\right) = \pi \left(\frac{D}{2}\right)^2 \qquad (4)$$

where A is the area of the ellipse and circle, x and y are apparent sizes of short axis and long axis of the ellipse and D is the apparent diameter of equal area circle as shown in Figure 3-3.

Therefore, FWHM of profile was considered as the apparent sizes of the selected profile line. Then the apparent sizes of long axis and short axis were obtained

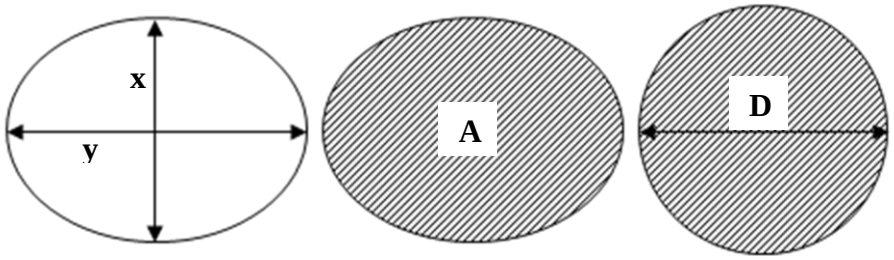

Figure 3-3. Estimation of real nodule size

for each selected nodules. Assuming the shape of the nodule is an ellipse, the area of the ellipse was calculated by using the measured apparent sizes of axes. Then the apparent diameter (D) of the equal area circle was obtained by using the Equation (4). Then the true sizes corresponds to the each nodule can be obtained from the calibration curve for nodule size (Figure 3-2).

Density of each real nodule needed to apply in simulation process. Densities appears in the images are apart from the true densities of the object. Therefore, there should also be criteria to find the true density of real nodules on images. Term ΔCT was defined as the density difference between background and the object function. This study has applied the ΔCT values instead of the density therefore; true values of ΔCTs were needed to calculate from images. Flowchart in Figure 3-4 shows the steps of the density calculation.

First the image simulation was done for the object function sizes from 3 to 10 mm. Apparent density percentage is defined as the percentage of the object function density appears on the center of the simulated nodule. Then the apparent density

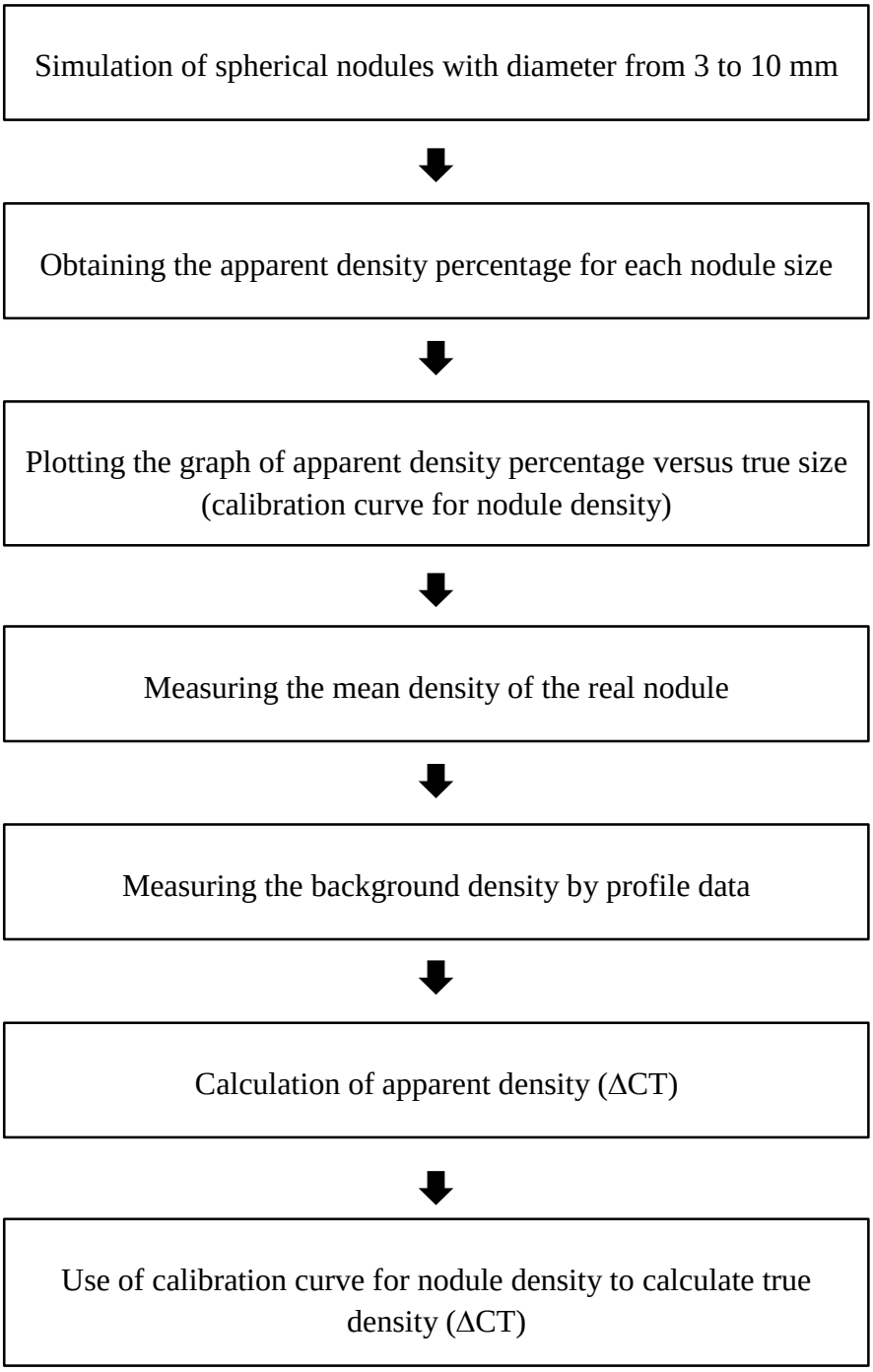

Figure 3-4. Flowchart of the nodule density measurement

percentage was obtained for each nodule size. Then the graph of apparent density percentage versus true size was obtained for simulated nodules [53]. Apparent density percentages for nodule sizes up to 10 mm can be obtained from the graph. Therefore,

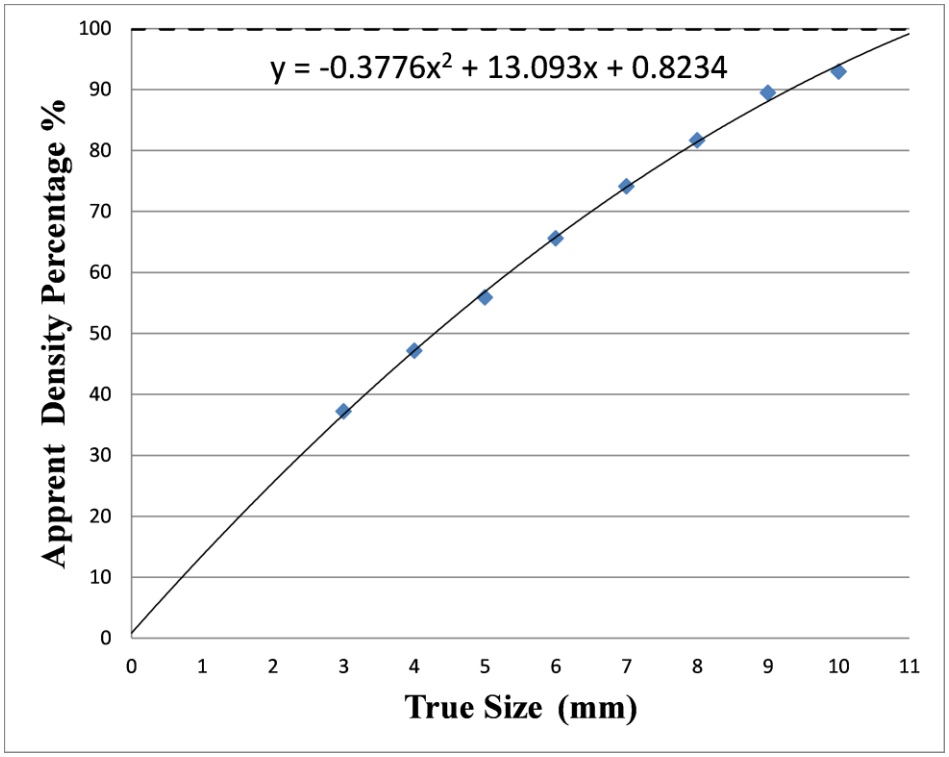

Figure 3-5. Calibration curve for nodule density

this can be considered as the calibration curve for nodule density. Then the mean density of each real nodule was measured by selecting small circular reign of interest near the nodule center. After that background densities of the screening images were obtained by profile data. ΔCT values were calculated by using the measured mean density and the background density. Calculated values are the density difference between the real nodule and the background appears in the image and these are apart from the true values. Then the graph of apparent density percentage versus the true size was obtained (Figure 3-5). Apparent density percentage for a given real nodule

size can be calculate from the graph. Therefore this can be considered as the calibration curve for nodule density. Next the calibration curve for nodule density was used to obtain the corresponding apparent density percentages for the each true nodule sizes calculated previously. Then the true densities (ΔCT) of each real nodule were calculated by using the Equation (5). Sizes of each nodule were calculated previously therefore, apparent density percentages can be obtained for each calculated nodule size from the calibration curve for nodule density (Figure 3-5).

$$\text{True Density}(\Delta\text{CT}) = \frac{\text{Mean Density } (\Delta\text{CT})}{\text{Apparent Density Percentage \%}} \qquad (5)$$

After that the corresponding nodules were simulated by applying the true sizes and densities (ΔCT values) and measured PSF and SSP values from the screening clinic to the object function [as in Equation (1)]. For the accuracy simulated images were computed with a fine digital sampling pitch (the interval of the discrete data). However, clinical images do not have such fine intervals as in simulated images. Superimposing process needs the similar intervals on both simulated and screening

(a) (b) (c)

Figure 3-6. Generation of virtual nodules. (a) Numerically generated object function with a fine digital sampling pitch. (b) Computed simulated blurred image. (c) Resampled image.

images for simple addition. Therefore, resampling should be performed before superimposing the simulated images on clinical images. Then, the simulated blurred images were transformed into same voxel size used in practical images that can be used in clinical evaluations. Figure 3-6 illustrates the three images of each stage starting from object function to resampled image. Superimposing the resampled 3D simulated images on practical screening images PSF-based virtual nodules are obtained. In this study the resampled images were superimposed on corresponding clinical images. Sample images for three selected cases are shown in Figure 3-7. Locations of the virtual nodules were decided considering the similar background including the location of blood vessels and distance to blood vessels. These images were analyzed by the prototype CAD system developed by our research team. Finally CAD outputs were taken and two separate FROC curves were obtained for real nodules and PSF-based virtual nodules.

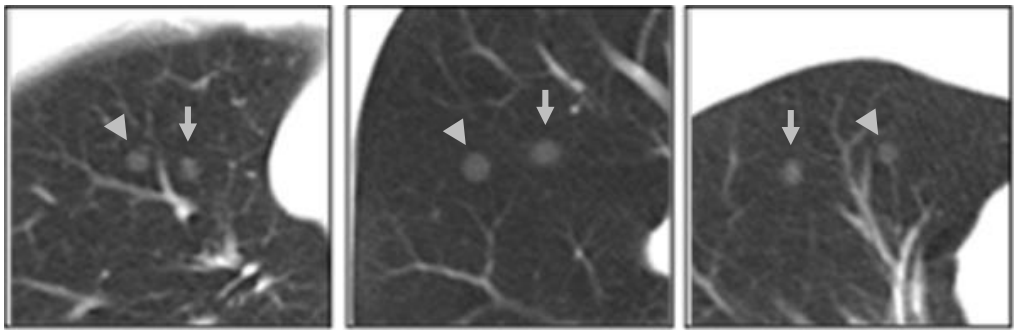

Figure 3-7. Selected three cases for real nodule and virtual nodules. Arrows are pointed to real nodules and arrowheads are pointed to virtual nodules.

3. 3. Results

Range of the applied nodule diameters was from 4.2 to 7.6 mm (mean 5.9 ± 1.0 mm) and the range of densities (ΔCT) was 194 to 790 HU (mean 382.2 ± 157.8 HU). Details of size and density measurements of each nodule have given in Table 3-1. Sample results of CAD system detections are shown in Figure 3-8.This CAD system indicates detected areas on the images by rectangles. These detected areas are either true positive (TP) or a false positive (FP). Here there are three detections, two TPs of

Figure 3-8. Sample detections by the CAD system. Arrows from left to right shows the detections of PSF-based virtual nodule, real nodule and a false positive respectively

real nodule and PSF-based virtual nodule and a FP. Based on detection results FROC curves are obtained. Two FROC curves for real nodules and PSF-based virtual nodules are shown in Figure 3-9.

Table 3-1. Measurement details of nodule size and density

Case Number	Short Axis x (mm)	Long Axis y (mm)	Apparent Size (mm)	True Size (mm)	Background Density (HU)	Mean Density (HU)	Apparent (ΔCT) (HU)	True (ΔCT) (HU)
5404	2.83	4.40	3.53	4.47	-955	-788	167	326
5330	5.36	5.03	5.20	6.53	-989	-791	198	282
5113	4.22	4.86	4.53	5.71	-907	-756	151	241
4884	4.56	6.73	5.54	6.96	-760	-426	334	452
3719	4.72	5.64	5.16	6.49	-952	-597	355	508
3917	4.04	2.73	3.32	4.22	-883	-498	385	790
3917	3.92	4.18	4.05	5.12	-929	-702	227	397
4067	5.26	6.49	5.84	7.34	-961	-808	153	199
4572	4.42	3.96	4.18	5.28	-950	-763	187	318
5373	4.18	4.30	4.24	5.35	-961	-588	373	627
5440	3.67	6.20	4.77	6.00	-878	-493	385	587
5599	4.33	4.08	4.20	5.31	-933	-723	210	356
5698	3.35	5.52	4.30	5.42	-858	-611	247	412
5986	5.61	6.09	5.84	7.34	-976	-806	170	220
6017	3.67	4.74	4.17	5.27	-912	-697	215	366
6084	5.10	4.41	4.74	5.97	-955	-781	174	268
6147	5.68	5.00	5.33	6.70	-926	-677	249	347
6284	3.59	3.80	3.69	4.67	-931	-674	257	485
15114	6.23	5.84	6.03	7.58	-920	-754	166	194

Results verify that CAD system for lung cancer CT screening has shown nearly similar performance on real nodules and PSF-based virtual nodules. Therefore, proposed PSF-based virtual nodule can be used as a substitute for real lung nodules for CAD system for lung cancer CT screening

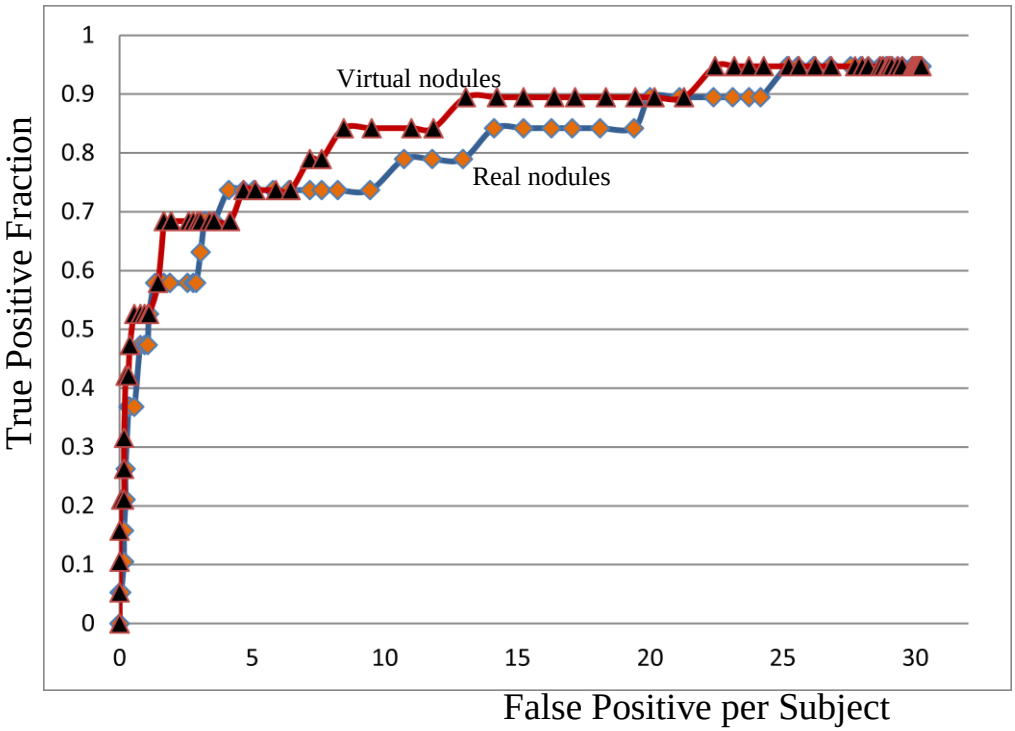

Figure 3-9. FROC curves for real nodules and PSF-based virtual nodules

.

3. 4. Discussion

This study has verified the use of PSF-based virtual nodules and real lung nodules with the lung cancer CT screening CAD system. CAD performance assessment required a larger number of different characteristic nodules. However, collection of such a large pool of diagnosed images need to made strenuous efforts and would be a laborious work in clinical practice. Therefore PSF-based virtual nodules would be a possible solution for CAD developers to assess the performances such as dependency on nodule characteristic and scan/reconstruction parameters. Furthermore, these virtual nodules could be used in QA process as well. Clinical images were selected from a dataset of a screening clinic and the one selection criteria was the appearance of nodule is nearly spherical or elliptical. There were about 80% nodules having such shape among the nodule size lower than 8 mm. There were about 75% nodules having diameter less than 8 mm in the clinical data set. Therefore, application of spherical nodules is comparable with the small lung nodules studies. This part of the study has proved the validity of using PSF-based virtual nodules for assessing the performance of lung cancer CT screening CAD system and therefore, validates the use of virtual nodules for QA process of CAD.

Chapter 4 CAD Performance with different conditions

4.1. CAD of different nodule sizes

4.1.1. Introduction

Clinically, the size and density of lung nodules are primary factors in determining the risk of malignancy. Several publications on CT screening for lung cancer have clearly demonstrated the positive relationship of lesion size to likelihood of malignancy [54, 55]. Lung cancer CT screening guidelines indicate that follow up actions are recommended for the subjects having nodules with diameters above 5 mm [56]. Therefore CAD performance dependence on nodule size is an important factor to be evaluated. The aim of this part of the study was to assess CAD performance dependence on virtual nodule size.

Nature of clinically detected lung nodules is complicated with irregular shape. Quantitative assessment of CAD performance for QA protocol needs a concrete definition for the nodule size. Therefore, in order to get clear definition for nodule size spherical object functions applied for the study. However, any irregular shape can be applied in the simulation process. Size dependency of CAD performance was analyzed by applying range from 4 to 8 mm in 1-mm increments. Each group consisted of a sufficiently large number of virtual nodules (150 nodules in 5 subjects). CAD analysis was performed and the detections were compared by using separate FROC curves for each nodule size.

4.1.2. Materials and Methods

Screening images of ten subjects which have not detected any lung nodules were selected from lung cancer CT screening dataset of General Hospital at Nagano, Japan. Approval of the institutional review board was taken from the same hospital. In this clinic, applicants have been subjected to lung screening examinations with a multidetector-row CT scanner without contrast enhancement (Asteion, Toshiba Medical Systems, Tokyo, Japan). The imaging parameters were as follows: reconstruction kernel FC50, 120 kV, 30 mA tube current, 8.0 mm slice thickness, 4 detector rows, 0.75 s rotation time and a pitch factor of 1.375. Selection of cases were done as such that; first all subjects' images were analyzed by the lung cancer CT screening CAD system. Radiologist has confirmed that there is no lung nodule on images, however CAD marks some FP on images. Then subjects were placed in ascending ordered according to the number of FPs marked by the CAD system. After that the subjects were divided into five groups containing approximately equal number of subjects in each group so that there were five groups having FP detections comparatively, very high, high, average, low and very low. Then 2 subjects from each group selected for the study. Therefore, total of 10 subjects were selected for the study.

Computer simulated nodule images were generated applying different sizes of 4, 5, 6, 7 and 8 mm to the object function as in Equation (1) while the ΔCT value of the object function was kept unchanged at 300 HU. For the simulation process measured PSF and SSP were substituted in Equation (1). Subsequently, images were resampled, and were superimposed on above selected five subjects' images one from

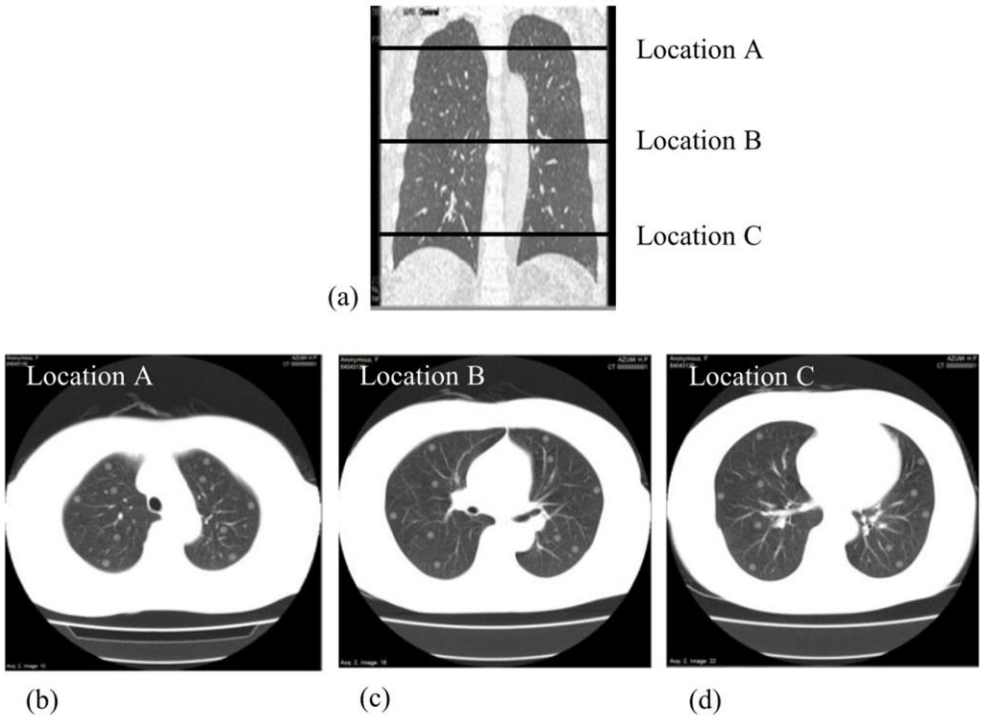

Figure 4-1 Virtual nodule images fused on three locations of the lung field. (a) Selected locations are shown in a coronal image of the lung field. (b) Location in the upper lung field. (c) Location in the middle lung field. (d) Location in the lower lung field.

each group. To cover the whole lung field, three locations were selected from the upper, middle and lower field areas as shown in Figure4-1. Each selected location was fused on 10 nodule images so that there were five virtual nodules in each of the left and right lungs. Thus, there were 30 virtual nodules per each subject with one size from 4 to 8 mm at a time. Five separate sets of images for the different nodule sizes were prepared. Each set of prepared screening images together with the rest of the five subjects' images (without virtual nodules) were separately analyzed by the CAD system. Prototype CAD system used in this study has provided the option of changing its sensitivity. Thus, nodule detection sensitivity of the system was changed, and the number of combinations of TP fraction (TPF) and FPs per subject (FPS) were taken for different sensitivity levels [41, 42]. These values were used to obtain FROC

curves. The jackknife FROC (JAFROC) method was used to estimate the statistical significance of the difference between the curves obtained for different nodule sizes separately [57].

4.1.3. Results

Performance dependence of a lung cancer CT screening CAD system has been assessed based on nodule size. Figure 4-2 shows sample CAD detections for different virtual nodule sizes. CAD performance dependence on nodule size has shown in the figure where all five virtual nodules having diameter of 8 mm have been detected but only four with diameter of 5 mm; thus one FN appears in Figure 4-2(a). Therefore, Figure 4-2 indicates that the CAD system detected larger virtual nodules than small ones. Overall results imply that tendency of virtual nodule detection by the CAD system can be seen towards larger-sized nodules.

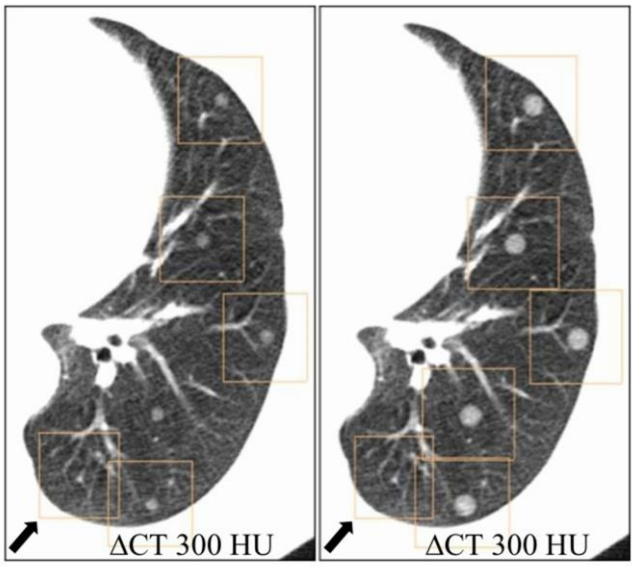

(a) diameter 5 mm (b) diameter 8 mm

Figure 4-2 CAD detections of virtual nodules having different sizes and same density (ΔCT = 300 HU) on a selected location. Arrow shows false positives on the bottom left of both images. (a) Only four virtual nodules with diameters of 5 mm were detected. (b) When the diameter is 8 mm, all five nodules were detected by CAD on the same location.

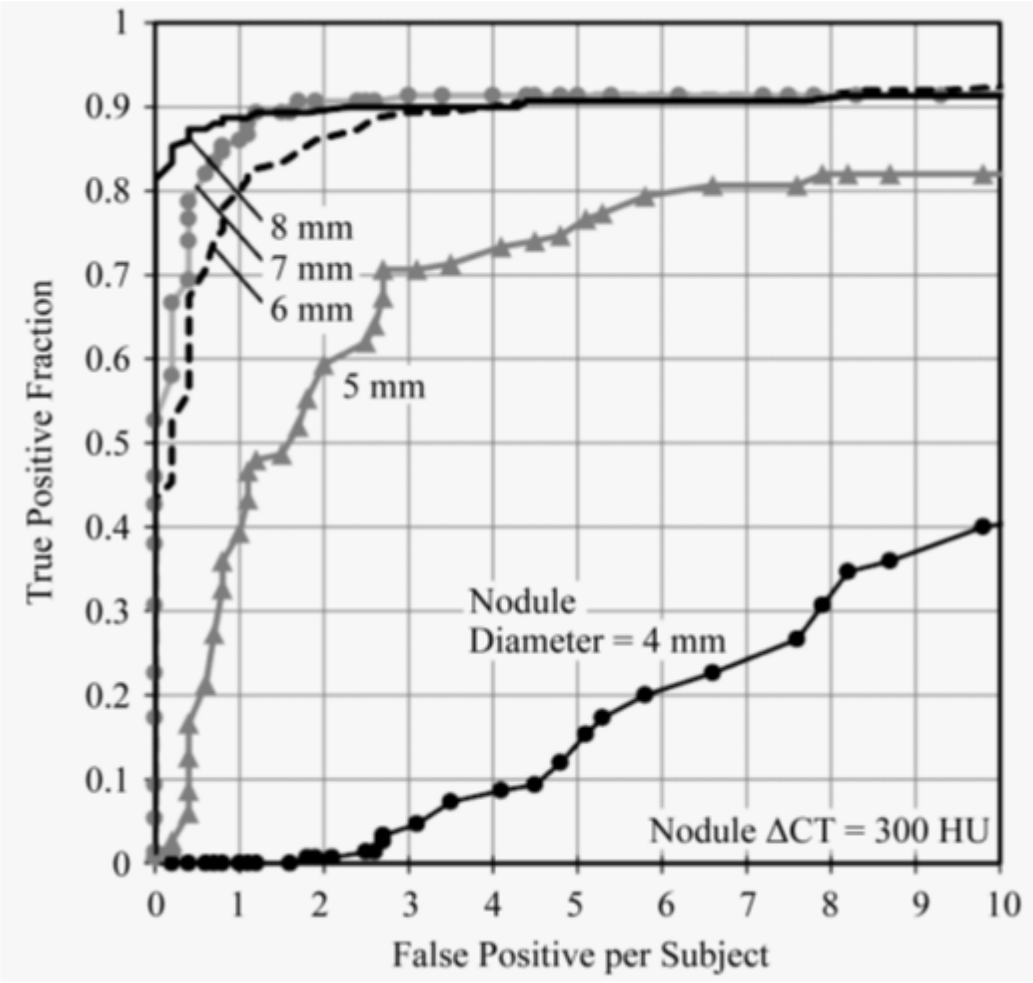

Figure 4-3. FROC curves for different nodule sizes from 4 - 8 mm. TPF of CAD detections increased with nodule size. However, when nodule size increased the gap between consecutive curves decreased.

Figure 4-3 shows FROC curves for CAD detections of different virtual nodule sizes. TPF of CAD detections of smaller-sized virtual nodules are lower than that of larger ones. The TPF for 4 mm virtual nodules is clearly the lowest value while other nodules are considerably high. TPFs increased with the increase of virtual nodule size. However, the gap between curves of consecutive virtual nodule sizes decreases when increasing their size. Results by the JAFROC method (Table 4-1) show that there are statistically significant differences between FROC curves of all pairs of different

virtual nodule sizes ($p < 0.05$) except between 7 and 8 mm curves ($p = 0.131$). According to these results, this CAD system was able to detect larger virtual nodules easily.

Table 4-1 p-Values for each pair of different nodule sizes

	4 mm	5 mm	6 mm	7 mm	8 mm
4 mm	-	< 0.05	< 0.001	< 0.001	< 0.001
5 mm	-	-	< 0.001	< 0.001	< 0.001
6 mm	-	-	-	<0.001	<0.05
7 mm	-	-	-	-	**0.131**
8 mm	-	-	-	-	-

4.1.4. Discussion

Performance of lung cancer CT screening CAD system has been assessed for various nodules sizes by applying PSF-based virtual nodules. Study conducted applying virtual nodules with sizes similar to the clinically proven actual nodule range [58]. Size of the virtual nodules has changed from 4 mm to 8 mm by 1 mm steps. This part of the study has conducted while keeping the nodule density (ΔCT) unchanged at 300 HU. Tested CAD system has shown poor performance on detection of 4 mm nodules. Nodules having diameter 5 mm or above have detected with more than 80% values for TPF. When the nodule size increases TPF also has increased, which is an acceptable result as a performance of CAD systems. Detailed results of CAD system performance dependence on nodule size have not yet been obtained by any other methods. Phantom studies permit only limited number of nodules set inside. This PSF-based method permits to apply multiple sizes to the various numbers of nodules. Therefore, PSF-based virtual nodule method allows assessing the detailed results of lung cancer CT screening CAD systems' performance dependence on nodule size.

4.2. CAD of different nodule densities

4.2.1. Introduction

Density of a lung nodule is also an important characteristic to be considered in lung cancer CT screening. Depending on the density lung nodules can be named as solid nodules and ground glass nodules. Some nodules contain high dense part as well as a low dense part called sub-solid nodules. Studies have shown the relationship of malignancy of lung nodule and the density. Therefore density of a nodule also plays an important role at decision making process in screening. The aim of this part of the study was to assess CAD performance dependence on virtual nodule density.

Clinically detected lung nodules are having heterogeneous density distribution with solid and sub-solid categories. In order to get a concrete definition in the quantitative assessment of CAD performance, this study has applied only one density nodule at selected time. Therefore, uniform density (ΔCT value) was applied to the object function as in Equation (1). For density dependency study simulated images were generated applying three different ΔCT value of 200, 300 and 400 HU to the object function. Finally FROC curves were plotted for CAD detections and statistically analyzed for different nodule densities.

4.2.2. Materials and Methods

Screening images of ten subjects were selected from the same hospital dataset as described in section 4.1.2. Three sets of computer simulated nodule images were generated applying uniform density for ΔCT values of 200, 300 and 400 HU. However, this simulation method can be used to apply complicated density distribution also. For the density dependency study size was kept unchanged at 6 mm.

Resampling and superimposing were performed as described earlier and three separate sets of images were prepared for each ΔCT value. Finally, the same procedure was followed for CAD detections, obtaining FROC curves and statistical analysis as in the previous section.

4.2.3. Results

Lung cancer CT screening CAD systems' performance has been assessed based on nodule density. Figure 4-4 shows sample CAD detections for different nodule

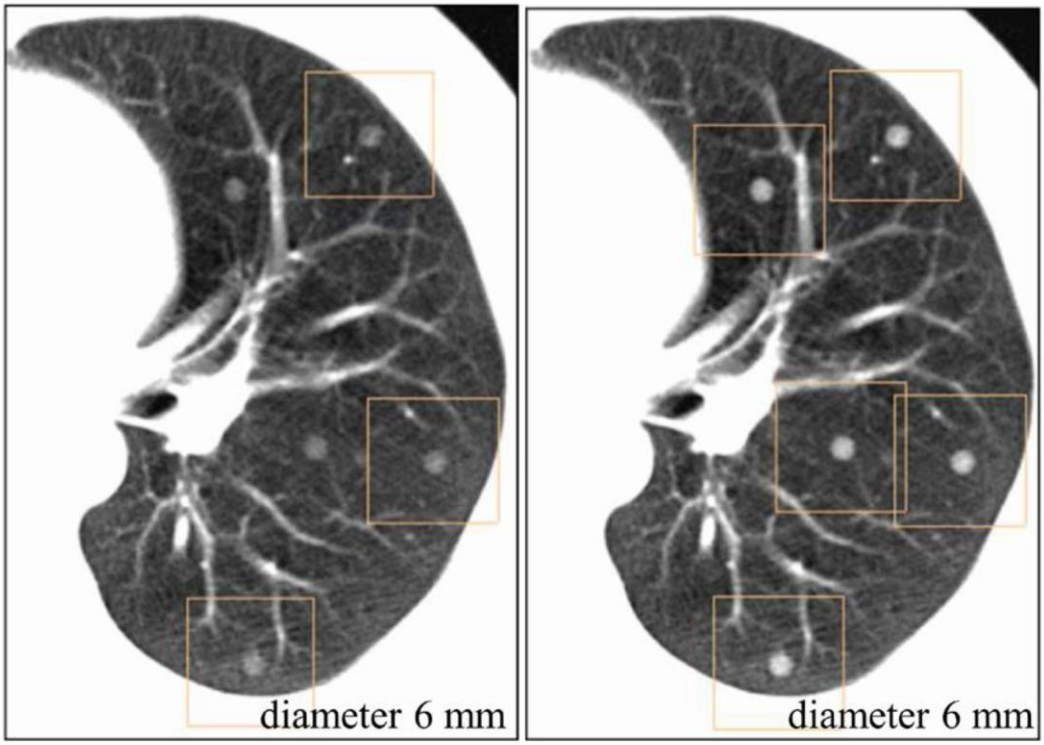

Figure 4-4. CAD detections of virtual nodules having different densities and same size (diameter 6 mm). (a) Only three virtual nodules with density (ΔCT) 200 HU were detected. (b) When the density (ΔCT) is 400 HU, all five nodules were detected on the same location.

densities. Nodule density affected on nodule detection by the CAD system (Figure 4-4). All five high density (ΔCT = 400 HU) nodules have been detected while only three from low density (ΔCT = 200 HU) nodules. Therefore, there are two false

negative (FN)s in Figure 4-4(a). Furthermore, the figure shows that a larger number of higher-density virtual nodules have been detected than low-density ones.

FROC curves of each density for ΔCT values of 200, 300 and 400 HU were plotted (Figure 4-5). The curves show that the lowest density (ΔCT = 200 HU) virtual nodules have the lowest TPF. The efficiency of CAD detection is shown to have increased with nodule density. Maximum TPFs of the 300 and 400 HU curves are more than 0.9 while the 200 HU curve has a value less than 0.9. The gap between FROC curves for a selected value of FPS decreased with density. CAD performance dependency on nodule density among the three densities was statistically analyzed by using the jackknife method (Table 4-2). Results show that a statistically significant difference can be seen between each nodule density ($p < 0.01$). Results show that more dense virtual nodules were conveniently detected by the tested CAD system.

Table 4-2. p-Values for each pair of different nodule densities (ΔCTs)

	200 HU	300 HU	400 HU
200 HU	-	< 0.001	< 0.001
300 HU	-	-	< 0.01
400 HU	-	-	-

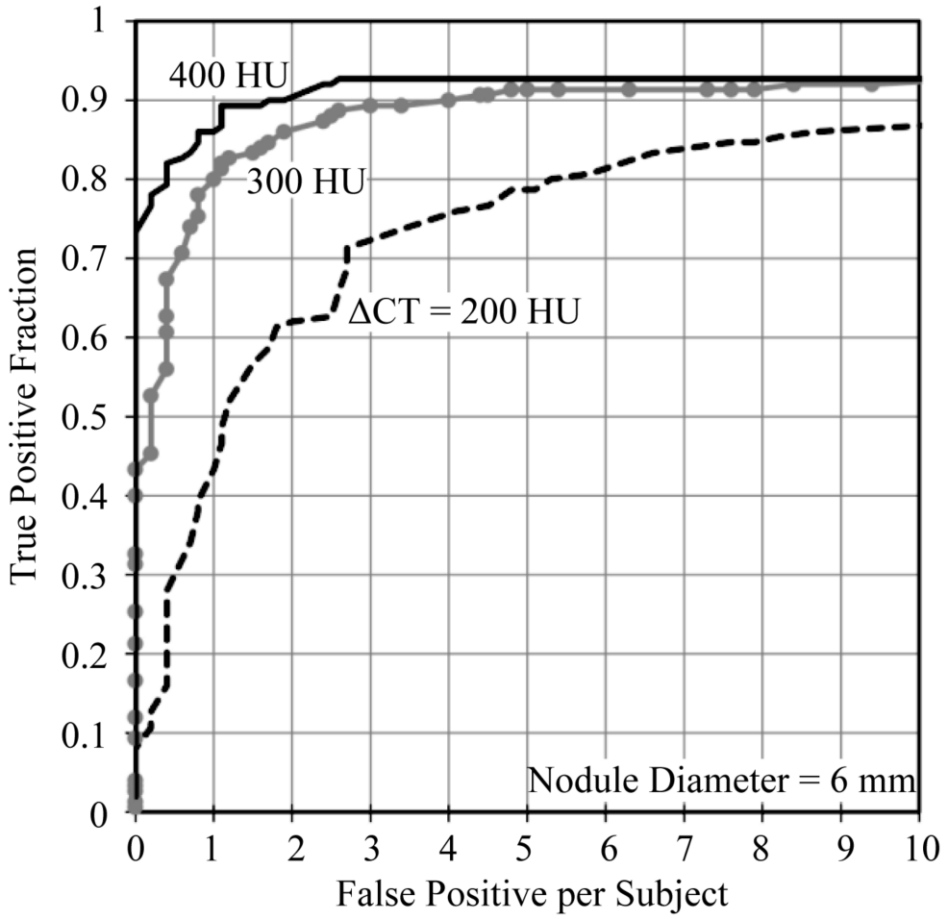

Figure 4-5. FROC curves for ΔCT values of 200, 300 and 400 HU. CAD showed better performance on 400 HU nodules. TPF increased with virtual nodule density. The gap between the 200 and 300 HU curves is higher than that of 300 and 400 HU. Curves have become horizontal when the FP per subject value is about eight

4.2.4. Discussion

Performance of lung cancer CT screening CAD system has been assessed by applying PSF-based virtual nodules having three different nodule densities. Study has conducted applying virtual nodules with density range similar to the clinically detected actual nodules [58]. Applied densities (ΔCT values) of virtual nodules were 200, 300 and 400 HU. Study has conducted while keeping the nodule size unchanged at 6 mm. Figure 4-5 shows that CAD system has shown good performance on nodules detection having TPF more than 80% for all three selected nodule densities. Nodules having the densities (ΔCT value) of 300 and 400 HU have been detected with 90% TPF. Furthermore, figure shows that, when the density increased detection rate also has increased. This is an acceptable result of nodule detection by a lung cancer CT screening CAD system. PSF-based virtual nodules are generated from uniform density object function. Therefore, density of the nodule is a known value and the detailed results of CAD performance dependence on nodule density can be obtained for certain densities. Clinically detected actual lung nodules may have heterogeneous density distribution and therefore assessing the CAD performance dependence on nodule density may not be possible for a given certain value of the density. PSF-based method permits to apply various densities to the larger numbers of virtual nodules. Therefore, detailed performance assessment of CAD could be performed by applying PSF-based virtual nodules.

4.3. CAD system performance with thin and thick slices

4.3.1. Introduction

Screening databases show that clinical practice of lung cancer CT screening applies different scan/reconstruction parameters. Slice thickness is one of them which use range of values from small to large values in different screening clinics. Standard for the slice thickness of lung cancer CT screening has not yet been set. Therefore, different institutes use slice thicknesses ranging from 1 to 10 mm. Application of CAD is possible with both thin and thick slices. Therefore it is important to assess the CAD performance for different slice thicknesses. Purpose of this part of study is to assess the CAD performance when using thin and thick slice images.

4.3.2. Materials and Methods

Screening images of two different screening hospitals were used for the study. One hospital has applied thin slice (1 mm) thickness and the other has applied thick slices (8 mm). Plaka Healthcare Center in Niigata has done the screening with thin slices. In this clinic, applicants have been subjected to lung cancer CT screening examinations with a multidetector-row CT scanner without contrast enhancement (Aquilion, Toshiba Medical Systems, Tokyo, Japan). The imaging parameters were as follows: reconstruction kernel FC51, 120 kV, 60 mA tube current, 1.0 mm slice thickness, 16 detector rows, 0.5 s rotation time and a pitch factor of 0.9375. Approval of the institutional review board was taken for accessing the database. Thick slices were selected from database of General Hospital at Nagano. In this hospital screenings have done with a multidetector-row CT scanner without contrast enhancement (Asteion, Toshiba Medical Systems, Tokyo, Japan). The imaging parameters were

similar to as in section 3.2. Sets of screening images were selected from both clinics as described in section 4.1.2. PSF and SSP of both clinics was measured and used in simulation process. Two separate sets of computer simulated nodule images were generated for the clinics. Applied density and diameter was same for both clinics as ΔCT value of 300 HU and object function diameter 6 mm. After that simulated nodules were resampled and superimposed on clinical images. Set of 150 nodules were applied on images of each case and the whole lung field was covered selecting three levels of the lung as described earlier. Finally, the same procedure was followed for CAD detections and obtaining FROC curves as in the previous sections.

4.3.3. Results

Lung cancer CT screening CAD systems' performance has been assessed for thin and thick slices. Figures 4-6 and 4-7 show sample CAD detections for thin and thick slices. According to Figure 4-6, four nodules from each left and right lungs have been detected by the CAD system on thin slice. Therefore, one false negative appears in each left and right lungs and the detection rate is 80%. Figure 4-7 shows that all five nodules on left lung have detected while four from the right lung. Therefore, one false negative appears in the selected location on thick slice and the detection rate is 90%. The figures show that tested CAD system has performed better with thick slices than thin slices.

FROC curves were plotted for CAD detections of both thin slices and thick slices. Figure 4-8 demonstrates that CAD system has maximum TPF about 0.8 for thin slices and 0.9 for thick slices. Therefore tested prototype CAD system has shown about 10% higher performance with thick slices than thin slices.

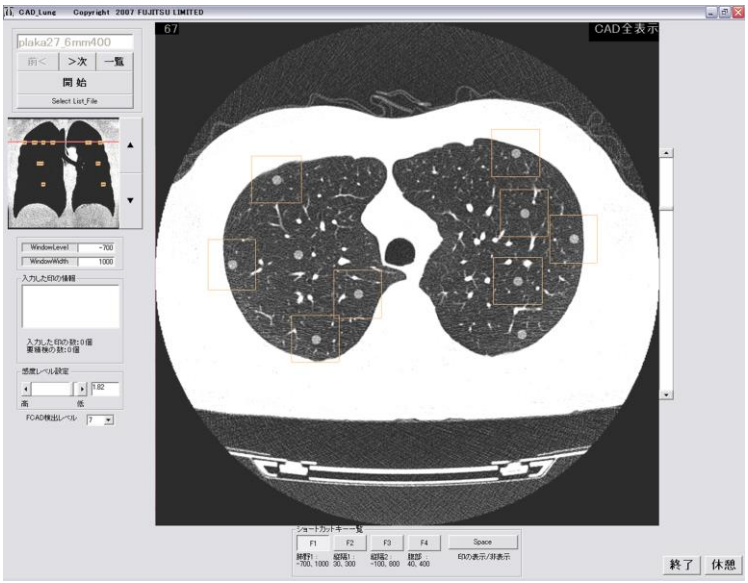

Figure 4-6.Sample nodule detection by CAD system on thin slices. Four nodules from left and right lungs are detected.

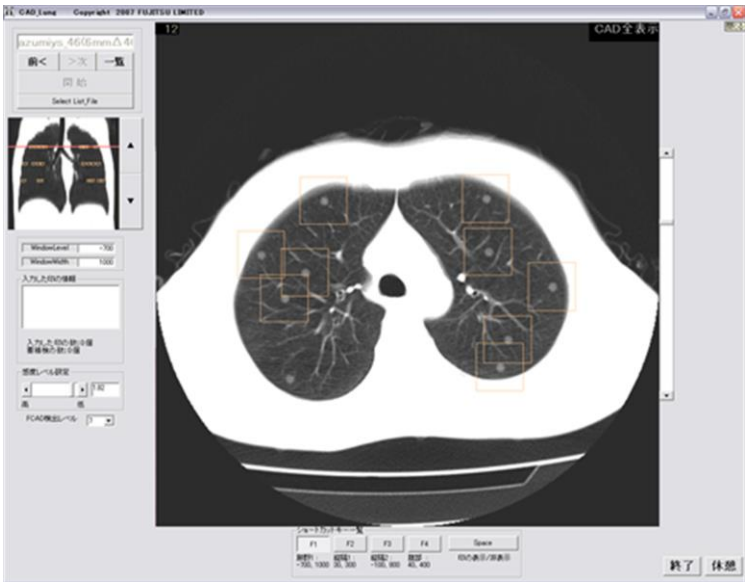

Figure 4-7. Sample nodule detection by CAD system on thick slices. All five nodules from left lung and only four from right lungs are detected.

4.3.4. Discussion

Performance of a lung cancer CT screening CAD system has assessed for thin and thick slices by applying PSF-based virtual nodules. Literature shows that lung cancer CT screening is performing for various scan/reconstruction conditions. Selection of slice thicknesses is considerable and it has changed from 1 to 10 mm [17 - 20, 35 - 43]. Generally a CAD system should be able to detect the nodules on both thin slices and thick slices. In clinical practice CAD may have to detect either nodules on thin slices or thick slices depending on the parameter selection of the clinic. This study has used thin slices with 1mm thickness from one clinic and thick slices with 8 mm thickness from next clinic and the performances are analyzed by FROC curves. Tested lung cancer CT screening CAD system has shown better performance with nodules on thick slices. FROC curves in Figure 4-8 shows that maximum TPF is about 90% for thick slices and about 80% for thin slices. Therefore, CAD system has shown about 10% higher performance with detecting nodules on thick slices. FROC curves for both thin and thin slices have become horizontal when the FP per subjects is about 7. These results were obtained by applying same nodule characteristics to each nodule having 6 mm diameter and 300 HU ΔCT value for the density. Therefore, PSF-based method can be used to assess the CAD performance with different slice thicknesses without an effect from nodule characteristics.

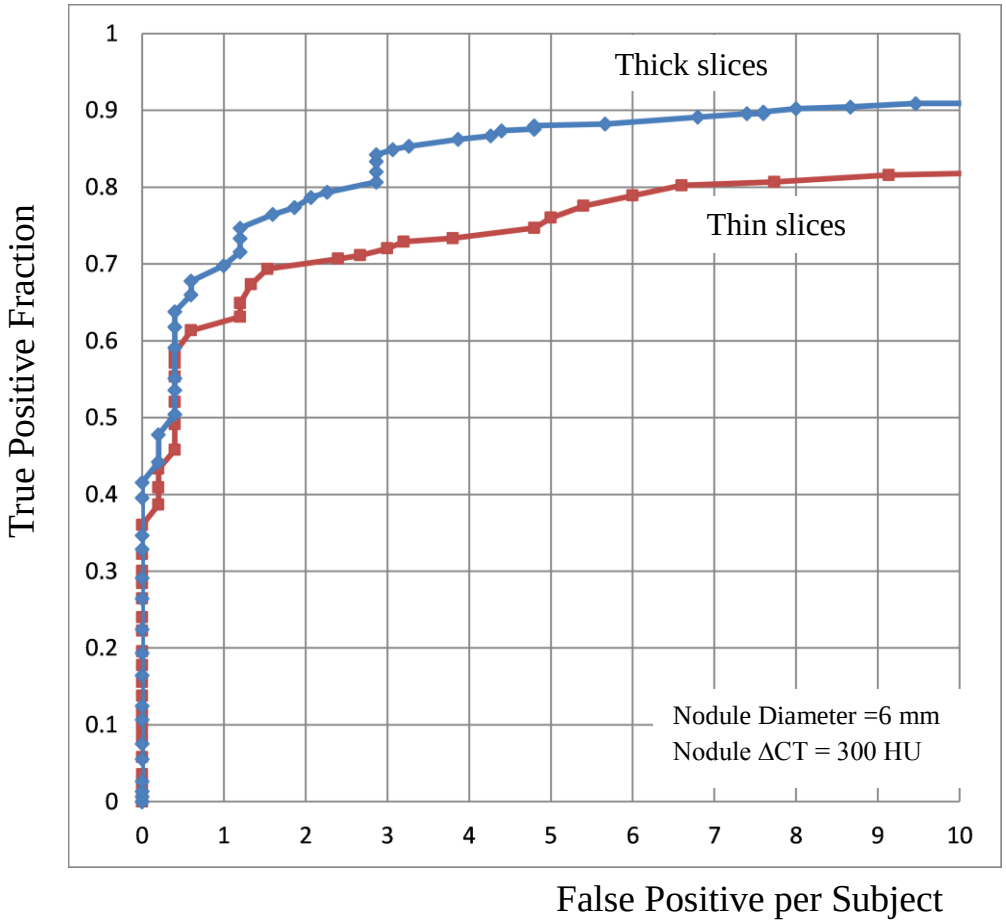

Figure 4-8. FROC curves for thin and thick slices. CAD has shown about 10% better performance on thick slices than thin slices. Curves have become horizontal when the FP per subject value is about eight

Chapter 5 Discussion

Performance of CAD system has been assessed in detail by applying PSF-based virtual nodules with verification. PSF-based virtual nodule method was used to obtain results with strong evidence of CAD performance on the same clinics' images with same scan/reconstruction conditions. Study in chapter 3 demonstrates the CAD system performance on real nodules and PSF-based virtual nodules. Similar FROC curves were obtained for both real nodules and the PSF-based virtual nodules. According to the obtained FROC curves, tested CAD system shows similar performance on detecting real nodules and proposed virtual nodules. This result suggests the validity of the use of PSF-based virtual nodules for CAD performance assessment and its QA.

Chapter 4 demonstrates the CAD performance dependence on nodule characteristic as well as scans parameters. First part of the study (section 4.1) shows the CAD performance dependence on nodule size. Size of a nodule is a critical factor in lung cancer CT screening. Screening guidelines are also prepared based on the size of lung nodules and the follow up actions are recommended for the nodules having diameter above 5 mm [56]. According to the results, CAD performance has increased with the nodule size. Study has shown acceptable results for CAD system performance. Second part of the study (section 4.2) based on the CAD performance dependence on nodule density. Results demonstrate that CAD performance increase with the nodule density.

These validated results show a detailed description on performance of lung cancer CT screening CAD system and also the results are generally expected.

Furthermore, detail results of CAD system performance dependence on nodule characteristics and scan/reconstruction conditions has not yet been obtained by any other method. Need of such method for QA purposes have been identified recently [44] and QA of CAD systems has become an active research field. Major objective of performing a QA test is to check the CAD performance consistence over the time. PSF-based virtual nodules based QA protocol is feasible to apply from initial implementation of a CAD system at a screening clinic (acceptance test) and routine QA test for assuring the consistency of CAD performance over time. Because of these reasons, I propose to apply PSF-based virtual nodules for QA of lung CAD system.

Proposed QA protocol includes number of steps from image simulation to analysis of CAD detections. Following flowchart (Figure 5-1) shows the main steps of the QA protocol for a CAD system at selected lung screening clinic. In the QA protocol, firstly the 2D PSF and the 1D SSP of the CT system at the screening clinic should be measured. Then lung nodule image simulation is performed based on the measured PSF and SSP. These measured PSF and SSP are substituted in the Equation (1). Therefore, this simulated image has the advantage of having an exact dependency on the characteristics of the spatial resolution of the same CT system [34]. Assuming solitary spherical pulmonary nodules object function O(x,y,z) is generated numerically with spherical shape and uniform density. Diameter of the object function was set at 6 mm for the proposed QA protocol. Screening guidelines has recommended by the Fleischner society mainly based on the nodule size. According to the guidelines follow up actions are required for the nodule size above 5 mm [56]. Therefore, 6 mm has selected as the nodule size for the proposed QA protocol. S.

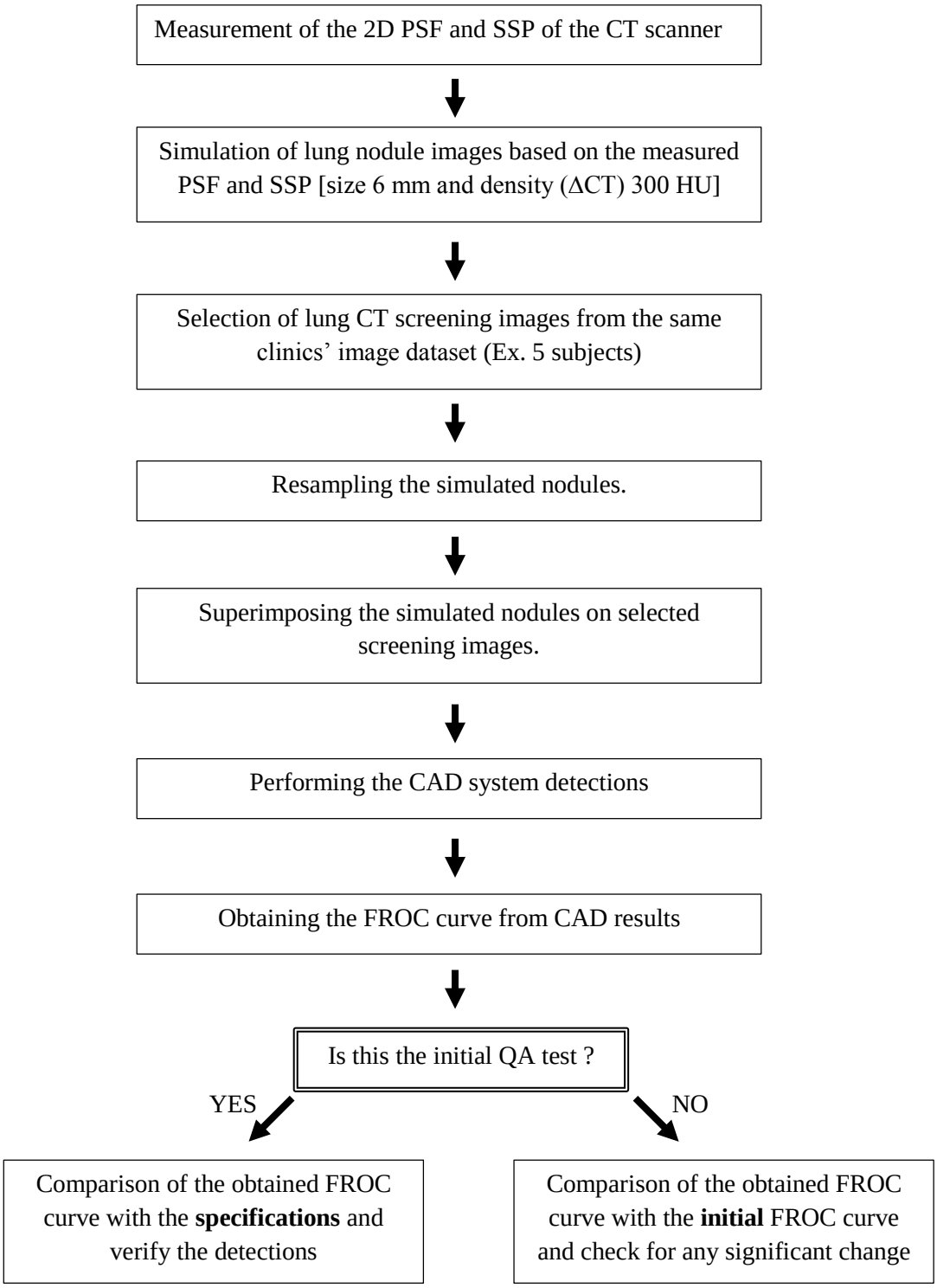

Figure 5-1 Flow of the QA protocol

Sone et al have published the density variation of tumors with size [58]. According to the published data, tumors with diameter 6 mm have average density about -600 HU. Therefore, proposed QA protocol applies nodule density -600 HU. According to the experience average density of the lung background is about -900 HU. Density of the object functions were assigned using the term ΔCT, (defined in section 3.2). Therefore the applied density (ΔCT) for the object function is 300 HU. Then lung CT screen images of five subjects from the same clinics' image dataset were selected for the QA protocol. Then images of healthy subjects on which radiologist have not detected any lung nodules are used for the QA test. For the accuracy simulated images were computed with a fine digital sampling pitch (the interval of the discrete data). However, clinical images do not have such fine intervals as in simulated images. Superimposing process needs the similar intervals on both simulated and screening images. Therefore, resampling should be performed before superimposing the simulated images on clinical images. Then, the simulated blurred images were transformed into practical images that can be used in clinical evaluations [59]. Figure 3-6 illustrates the three images of each stage starting from object function to resampled image. (a) Numerically generated object function with a fine digital sampling pitch. (b) Computed simulated blurred image. (c) Resampled image. Superimposing the resampled 3D simulated images on practical screening images PSF-based virtual nodules are obtained and these images are applied for the QA process. Locations of the nodules were selected covering the whole lung field as shown in Figure 4-1. Then the CAD detections should be performed and the FROC curves are obtained based on detection results. Then the results can be analyze either

with specifications given by the manufacturer or the initial QA test. If this is the initial QA test (i.e., the acceptance test), then the specifications given by the manufacturer and the obtained results are checked for any significant difference. If this is a routine QA test done for checking the consistence of CAD performance over time, then the initial result at the acceptance test and the obtained results are checked for any significant change.

This study has proposed a QA protocol for lung cancer CT screening CAD system. Recommendations for minimum number of cases and the set of reference nodules have not yet been published by any recognized body. Sufficiently large number of nodules is needed for QA process and therefore, it will take relatively longer period to collect such images for an individual clinic [44]. AAPM CAD subcommittee also has recognized that collection of large number of nodules is not practical for QA in all clinical sites. Image simulation would be a solution for this burden and multiple nodules with various densities can be simulated as required for a particular QA procedure. This study has proposed to apply total of 150 nodules superimposed on five healthy cases' images. Proposed size and the density (ΔCT) are 6 mm and 300HU. Selection of above parameters (number of cases, total number of nodules, nodule size and density) is arguable and open for discussion. However, all these parameters can be changed without extra effort with an agreement with evidence of relative parties or recognized body.

This study has some limitations. Firstly, study used only one CAD system however; it needs to apply with some other CAD systems also. Because CAD systems have many types of algorithms and therefore feasibility of the proposed method

should be checked with different systems. Secondly, simulated nodules were calculated from the object functions determined as ideal spheres with uniform density. Study has applied spherical nodules with uniform density. However, clinical nodules may have a complex shape with heterogeneous density [58, 59]. Including such complex nodules future studies should be conducted. Thirdly only three levels of the lung field have considered superimposing the virtual nodules and the locations of the nodule manually selected. Only five subjects' screening images were used for this study and therefore future studies can be performed increasing number of subjects and locations of the lung field.

Chapter 6 Conclusion

This study has proposed a new approach for QA of lung cancer CT screening CAD systems. Validity of the PSF-based virtual nodules for the use of CAD performance assessment was verified by comparing with clinical nodules. It was demonstrated that virtual nodule method allows assessing detailed results of the CAD system performance. The proposed method can be applied as a QA procedure for lung cancer CT screening CAD systems.

Reference list

1. Jemal A, Bray F, Center MM, Ferlay J, Ward E, Forman D. Global cancer statistics. CA Cancer J Clin. 2011 Mar-Apr;61(2):69-90.
2. International Early Lung Cancer Action Program Investigators, Henschke CI, Yankelevitz DF, Libby DM, Pasmantier MW, Smith JP, Miettinen OS. Survival of patients with stage I lung cancer detected on CT screening. N Engl J Med. 2006 Oct 26;355(17):1763-71.
3. Jeffers CD, Pandey T, Jambhekar K, Meek M. Effective use of low-dose computed tomography lung cancer screening. Curr Probl Diagn Radiol. 2013 Sep-Oct;42(5):220-30.
4. Siegel R, Naishadham D, Jemal A. Cancer statistics, 2013.CA: Cancer J Clin 2013;63(1):11–30.
5. Henschke CI. Early lung cancer action project: overall design and findings from baseline screening. Cancer. 2000 Dec 1;89(11 Suppl):2474-82.
6. Van Klaveren RJ, Oudkerk M, Prokop M, Scholten ET, Nackaerts K, Vernhout R, van Iersel CA, van den Bergh KA, van 't Westeinde S, van der Aalst C, Thunnissen E, Xu DM, Wang Y, Zhao Y, Gietema HA, de Hoop BJ, Groen HJ, de Bock GH, van Ooijen P, Weenink C, Verschakelen J, Lammers JW, Timens W, Willebrand D, Vink A, Mali W, de Koning HJ. Management of lung nodules detected by volume CT scanning. N Engl J Med. 2009 Dec 3;361(23):2221-9.
7. National Lung Screening Trial Research Team, Aberle DR, Berg CD, Black WC, Church TR, Fagerstrom RM, Galen B, Gareen IF, Gatsonis C, Goldin J,

Gohagan JK, Hillman B, Jaffe C, Kramer BS, Lynch D, Marcus PM, Schnall M, Sullivan DC, Sullivan D, Zylak CJ. The National Lung Screening Trial: overview and study design. Radiology. 2011 Jan;258(1):243-53. doi: 10.1148.

8. National Lung Screening Trial Research Team, Aberle DR, Adams AM, Berg CD, Black WC, Clapp JD, Fagerstrom RM, Gareen IF, Gatsonis C, Marcus PM, Sicks JD. Reduced lung-cancer mortality with low-dose computed tomographic screening. N Engl J Med. 2011 Aug 4;365(5):395-409.

9. Iinuma T, Tateno Y, Matsumoto T, Yamamoto S, Matsumoto M. Preliminary specification of X-ray CT for lung cancer screening (LSCT) and its evaluation on risk-cost-effectiveness. Nihon Igaku Hoshasen Gakkai Zasshi. 1992 Feb 25;52(2):182-90.

10. Sone S, Takashima S, Li F, Yang Z, Honda T, Maruyama Y, Hasegawa M, Yamanda T, Kubo K, Hanamura K, Asakura K. Mass screening for lung cancer with mobile spiral computed tomography scanner. Lancet. 1998 Apr 25;351(9111):1242-5.

11. Kaneko M, Eguchi K, Ohmatsu H, Kakinuma R, Naruke T, Suemasu K, Moriyama N. Peripheral lung cancer: screening and detection with low-dose spiral CT versus radiography. Radiology. 1996 Dec;201(3):798-802.

12. Sone S, Li F, Yang ZG, Honda T, Maruyama Y, Takashima S, Hasegawa M, Kawakami S, Kubo K, Haniuda M, Yamanda T. Results of three-year mass screening programme for lung cancer using mobile low-dose spiral computed tomography scanner. Br J Cancer. 2001 Jan 5;84(1):25-32.

13. Whitson BA, Groth SS, Duval SJ, Swanson SJ, Maddaus MA. Surgery for early-stage non-small cell lung cancer: a systematic review of the video-assisted thoracoscopic surgery versus thoracotomy approaches to lobectomy. Ann Thorac Surg. 2008 Dec;86(6):2008-16; discussion 2016-8.

14. Ostroff JS, Buckshee N, Mancuso CA, Yankelevitz DF, Henschke CI. Smoking cessation following CT screening for early detection of lung cancer. Prev Med. 2001 Dec;33(6):613-21.

15. Jett JR, Midthun DE. Screening for lung cancer: for patients at increased risk for lung cancer, it works. Ann Intern Med. 2011 Oct 18;155(8):540-2.

16. Kanazawa K, Kawata Y, Niki N, Satoh H, Ohmatsu H, Kakinuma R, Kaneko M, Moriyama N, Eguchi K. Computer-aided diagnosis for pulmonary nodules based on helical CT images. Comput Med Imaging Graph. 1998 Mar-Apr;22(2):157-67.

17. Das M, Mühlenbruch G, Heinen S, Mahnken AH, Salganicoff M, Stanzel S, Günther RW, Wildberger JE. Performance evaluation of a computer-aided detection algorithm for solid pulmonary nodules in low-dose and standard-dose MDCT chest examinations and its influence on radiologists. Br J Radiol. 2008 Nov;81(971):841-7.

18. Way T, Chan HP, Hadjiiski L, Sahiner B, Chughtai A, Song TK, Poopat C, Stojanovska J, Frank L, Attili A, Bogot N, Cascade PN, Kazerooni EA. Computer-aided diagnosis of lung nodules on CT scans: ROC study of its effect on radiologists' performance. Acad Radiol. 2010 Mar;17(3):323-32.

19. Roos JE, Paik D, Olsen D, Liu EG, Chow LC, Leung AN, Mindelzun R, Choudhury KR, Naidich DP, Napel S, Rubin GD. Computer-aided detection (CAD) of lung nodules in CT scans: radiologist performance and reading time with incremental CAD assistance. Eur Radiol. 2010 Mar;20(3):549-57.

20. Zhao Y, de Bock GH, Vliegenthart R, van Klaveren RJ, Wang Y, Bogoni L, de Jong PA, Mali WP, van Ooijen PM, Oudkerk M. Performance of computer-aided detection of pulmonary nodules in low-dose CT: comparison with double reading by nodule volume. Eur Radiol. 2012 Oct; 22(10):2076-84.

21. Lusted LB. Logical analysis in roentgen diagnosis. Radiology. 1960 Feb;74:178-93.

22. Tuddenham WJ. Visual search, image organization, and reader error in roentgen diagnosis. Studies of the psycho-physiology of roentgen image perception. Radiology. 1962 May;78:694-704.

23. Kundel HL, Revesz G. Lesion conspicuity, structured noise, and film reader error. AJR Am J Roentgenol. 1976 Jun;126(6):1233-8.

24. Berbaum KS, Franken EA, Dorfman DD, Rooholamini SA, Kathol MH, Barloon TJ, Behlke FM, Sato Y, Lu CH, Elkhoury GY, Flickinger FW, and Montgomery WJ. Satisfaction of search in diagnostic-radiology. Invest Radiol. 1990 Feb;25(2):133-40.

25. Renfrew DL, Franken EA Jr, Berbaum KS, Weigelt FH, Abu-Yousef MM. Error in radiology: classification and lessons in 182 cases presented at a problem case conference. Radiology. 1992 Apr;183(1):145-50.

26. Petrick N, Sahiner B, Armato SG 3rd, Bert A, Correale L, Delsanto S, Freedman MT, Fryd D, Gur D, Hadjiiski L, Huo Z, Jiang Y, Morra L, Paquerault S, Raykar V, Samuelson F, Summers RM, Tourassi G, Yoshida H, Zheng B, Zhou C, Chan HP. Evaluation of computer-aided detection and diagnosis systems. Med Phys. 2013 Aug;40(8):087001.

27. Doi K. Current status and future potential of computer-aided diagnosis in medical imaging. Br J Radiol 2005;78 Spec No 1:S3-S19.

28. Giger ML, Suzuki K. Computer-Aided Diagnosis (CAD) In: Feng DD. eds. Biomedical Information Technology. Academic Press, 2007:359-74.

29. Doi K. Computer-aided diagnosis in medical imaging: historical review, current status and future potential. Comput Med Imaging Graph 2007;31:198-211.

30. Giger ML, Chan HP, Boone J. Anniversary paper: History and status of CAD and quantitative image analysis: the role of Medical Physics and AAPM. Med Phys. 2008 Dec;35(12):5799-820.

31. Suzuki K, A review of computer-aided diagnosis in thoracic and colonic imaging, Quant Imaging Med Surg 2012; 2(3):163-176.

32. Winsberg F, Elkin M, Macy J Jr, et al. Detection of radiographic abnormalities in mammograms by means of optical scanning and computer analysis. Radiology 1967;89:211-5.

33. Li F, Arimura H, Suzuki K, Shiraishi J, Li Q, Abe H, Engelmann R, Sone S, MacMahon H, Doi K. Computer-aided detection of peripheral lung cancers

missed at CT: ROC analyses without and with localization. Radiology. 2005 Nov;237(2):684-90.

34. Marasinghe JC, Ohkubo M, Kobayashi H, Murao K, Matsumoto T, Sone S, Wada S. Feasible method to assess the performance of a lung cancer CT screening CAD system in clinical practice: dependence on nodule size and density. International Journal of Medical Physics, Clinical Engineering and Radiation Oncology 2014, 3, 107-116.

35. Lee Y, Hara T, Fujita H, Itoh S, Ishigaki T. Automated detection of pulmonary nodules in helical CT images based on an improved template-matching technique. IEEE Trans Med Imaging. 2001 Jul;20(7):595-604.

36. Awai K, Murao K, Ozawa A, Komi M, Hayakawa H, Hori S, Nishimura Y. Pulmonary nodules at chest CT: effect of computer-aided diagnosis on radiologists' detection performance. Radiology. 2004 Feb;230(2):347-52.

37. Li Q, Li F, Doi K. Computerized detection of lung nodules in thin-section CT images by use of selective enhancement filters and an automated rule-based classifier. Acad Radiol. 2008 Feb;15(2):165-75.

38. Retico A, Delogu P, Fantacci ME, Gori I, Preite Martinez A. Lung nodule detection in low-dose and thin-slice computed tomography. Comput Biol Med. 2008 Apr; 38(4):525-34.

39. Sahiner B, Chan HP, Hadjiiski LM, Cascade PN, Kazerooni EA, Chughtai AR, Poopat C, Song T, Frank L, Stojanovska J, Attili A. Effect of CAD on radiologists' detection of lung nodules on thoracic CT scans: analysis of an

observer performance study by nodule size. Acad Radiol. 2009 Dec;16(12):1518-30.

40. Messay T, Hardie RC, Rogers SK. A new computationally efficient CAD system for pulmonary nodule detection in CT imagery. Med Image Anal. 2010 Jun;14(3):390-406.

41. Takizawa, H., Yamamoto, S. and Shiina, T. Recognition of pulmonary nodules in thorasic ct scans using 3-d deformable object models of different classes. Algorithms, 2010 10, 125-144.

42. Kusano S, Nakagawa T, Aoki T, Nawa T, Nakashima K, Goto Y, Korogi Y. Efficacy of computer-aided diagnosis in lung cancer screening with low-dose spiral computed tomography: receiver operating characteristic analysis of radiologists' performance. Jpn J Radiol. 2010 Nov;28(9):649-55.

43. Cascio D, Magro R, Fauci F, Iacomi M, Raso G. Automatic detection of lung nodules in CT datasets based on stable 3D mass-spring models. Comput Biol Med. 2012 Nov;42(11):1098-109.

44. Huo Z, Summers RM, Paquerault S, Lo J, Hoffmeister J, Armato SG 3rd, Freedman MT, Lin J, Lo SC, Petrick N, Sahiner B, Fryd D, Yoshida H, Chan HP. Quality assurance and training procedures for computer-aided detection and diagnosis systems in clinical use. Med Phys. 2013 Jul;40(7):077001.

45. Boone JM., Cody DD., Fisher JR., Frey GD, Glasser Hy, Gray J, Haus AG., Hefner LV., Holmes RL., Kobistek RJ., Ranallo FN.,. Rauch PL, Rossi RP., Seibert J. A, Keith J. , Suleiman OH., Schenck JR., Thompson S K., Quality control in diagnostic radiology, AAPM report number 74.

46. Polacin A, Kalender WA, Brink J, Vannier MA. Measurement of slice sensitivity profiles in spiral CT. Med Phys. 1994 Jan;21(1):133-40.

47. Prevrhal S, Fox JC, Shepherd JA, Genant HK. Accuracy of CT-based thickness measurement of thin structures: modeling of limited spatial resolution in all three dimensions. Med Phys. 2003 Jan;30(1):1-8.

48. Rollano-Hijarrubia E, Stokking R, van der Meer F, Niessen WJ. Imaging of small high-density structures in CT A phantom study. Acad Radiol. 2006 Jul;13(7):893-908.

49. Ohkubo M, Wada S, Matsumoto T, Nishizawa K. An effective method to verify line and point spread functions measured in computed tomography. Med Phys. 2006 Aug;33(8):2757-64.

50. Ohkubo M, Wada S, Ida S, Kunii M, Kayugawa A, Matsumoto T, Nishizawa K, Murao K. Determination of point spread function in computed tomography accompanied with verification. Med Phys. 2009 Jun;36(6):2089-97.

51. Ohkubo M, Wada S, Kayugawa A, Matsumoto T, Murao K. Image filtering as an alternative to the application of a different reconstruction kernel in CT imaging: feasibility study in lung cancer screening. Med Phys. 2011 Jul;38(7):3915-23.

52. Godoy MC, Kim TJ, White CS, Bogoni L, de Groot P, Florin C, Obuchowski N, Babb JS, Salganicoff M, Naidich DP, Anand V, Park S, Vlahos I, Ko JP. Benefit of computer-aided detection analysis for the detection of subsolid and solid lung nodules on thin- and thick-section CT. AJR Am J Roentgenol. 2013 Jan;200(1):74-83.

53. Ohkubo M, Wada S, Kunii M, Matsumoto T, Nishizawa K. Imaging of small spherical structures in CT: simulation study using measured point spread function. Med Biol Eng Comput. 2008 Mar;46(3):273-82.

54. Midthun DE, Swensen SJ, Jett JR, Hartman TE. Evaluation of nodules detected by screening for lung cancer with low dose spiral computed tomography. Lung Cancer 2003;41.

55. Henschke CI, Yankelevitz DF, Naidich DP, McCauley DI, McGuinness G, Libby DM, Smith JP, Pasmantier MW, Miettinen OS. CT screening for lung cancer: suspiciousness of nodules according to size on baseline scans. Radiology. 2004 Apr;231(1):164-8. Epub 2004 Feb 27.

56. Naidich DP, Bankier AA, MacMahon H, Schaefer-Prokop CM, Pistolesi M, Goo JM, Macchiarini P, Crapo JD, Herold CJ, Austin JH, Travis WD. Recommendations for the management of subsolid pulmonary nodules detected at CT: a statement from the Fleischner Society. Radiology. 2013 Jan;266(1):304-17.

57. Chakraborty DP. A brief history of free-response receiver operating characteristic paradigm data analysis. Acad Radiol. 2013 Jul;20(7):915-9.

58. Sone S, Hanaoka T, Ogata H, Takayama F, Watanabe T, Haniuda M, Kaneko K, Kondo R, Yoshida K, Honda T. Small peripheral lung carcinomas with five-year post-surgical follow-up: assessment by semi-automated volumetric measurement of tumour size, CT value and growth rate on TSCT. Eur Radiol. 2012 Jan;22(1):104-19.

59. Ohno K, Ohkubo M, Marasinghe JC, Murao K, Matsumoto T, Wada S. Accuracy of lung nodule density on HRCT: analysis by PSF-based image simulation. J Appl Clin Med Phys. 2012 Nov 8; 13(6):3868.

Acknowledgement

I am grateful to all who helped me to complete this thesis successfully. In the first place, I am extremely grateful to my supervisor Prof. Shinichi Wada for his valuable guidance, encouragement, supports and cares throughout the course and stay in Japan. His challenges brought this work towards a successful completion. Also my special and heartily thanks go to my co-supervisor, Prof. Masaki Ohkubo for his support and giving me extra ordinary experiences throughout the work and stay in Japan. I also want to express my gratitude to Professor Masatoshi Saito for his support and encouragement.

My warmest thanks go to the examiners of the thesis Prof. Toshihiro Takahashi and Prof. Yongbum Lee for their valuable advices and comments for the thesis. I would like to express my sincere thanks to Mitsubishi Corporation Japan and HETC project Ministry of Higher education, Sri Lanka for the financial support and Fujitsu LTD. Japan for providing the lung cancer CT screening CAD system. This work was supported by JSPS KAKENHI grant numbers 25461803 and 26460722.

I would like to record my gratitude to former dean of the School of Health Science, Faculty of Medicine, Niigata University, Prof. Shigeki Hirano and Prof. Tsutomu Suzuki, Prof. Makoto Sakamoto and Prof. Naoshi Fujiwara. Special thanks go to Dr. T Matsumoto, Dr. S Niizuma and Prof. S Sone for their expert guidance and providing clinical images for the study. I would like to specially mention my heartfelt thanks to late Prof. Kahoru Tanno, Prof. Megumi Sato and Prof. Marcello Sato for their continuous support throughout the stay in Japan.

I also must note my deepest gratitude to my wife, mother and family for their continuous support and encouragement to achieve my educational aspirations.

Finally, I would like to record my gratitude to Takako sensei, Mr Hajime Kobayashi, Mr Akifumi Yoshida, Ms Menaka Hindagolla and my friends, colleagues and all the others who helped me directly and indirectly to success my doctoral study.

Publications Associated with This Thesis

Journal Articles

1. Ken Ohno, Masaki Ohkubo, **Janaka C. Marasinghe**, Kohei Murao, Toru Matsumoto, Shinichi Wada. Accuracy of lung nodule density on HRCT: analysis by PSF-based image simulation. JOURNAL OF APPLIED CLINICAL MEDICAL PHYSICS. 2012 Nov 8;13(6):3868. doi: 10.1120/jacmp.v13i6.3868.
2. Masaki Ohkubo, Shinichi Wada, Satoshi Kanai, Kazuhiro Ishikawa, **Janaka C. Marasinghe**, Toru Matsumoto. Observer-independent nodule-detectability index for low-dose lung cancer screening CT: a pilot study. Radiological Physics and Technology. 2013 Jul;6(2):492-9. doi: 10.1007/s12194-013-0225-2. Epub 2013 Jun 9.
3. **Janaka C. Marasinghe**, Masaki Ohkubo, Hajime Kobayashi, Kohei Murao, Toru Matsumoto, Shusuke Sone, Shinichi Wada. Feasible Method to Assess the Performance of a Lung Cancer CT Screening CAD System in Clinical Practice: Dependence on Nodule Size and Density. International Journal of Medical Physics, Clinical Engineering and Radiation Oncology 2014, 3: 107-116. doi:10.4236 /ijmpcero.2014.32016

Conference Papers

1. **Janaka C Marasinghe**, Masaki Ohkubo, Hajime Kobayashi, Kohei Murao, Toru Matsumoto, Shinji Niizuma , Shusuke Sone, Shinichi Wada. Performance assessment of CAD for lung cancer CT screening by applying PSF-based virtual nodules: Influence on slice thickness and nodule density. 104th Biannual Meeting of Japanese Society of Medical Physics, Tsukuba Japan, Japanese Journal of Medical Physics, Vol 32, Supplement No 3, September 2012: 139-140.
2. Hajime Kobayashi, Masaki Ohkubo, **Janaka C Marasinghe**, Kohei Murao, Toru Matsumoto, Shusuke Sone, Shinichi Wada. Performance assessment of CAD for lung cancer CT screening by applying PSF-based virtual nodules fusion onto screening CT images. 104th Biannual Meeting of Japanese Society of Medical Physics, Tsukuba Japan, Japanese Journal of Medical Physics, Vol 32, Supplement No 3, September 2012: 141-142.
3. **J C Marasinghe**, M Ohkubo, H Kobayashi, K Murao,T Matsumoto, S Niizuma , S Sone, S Wada. Application of PSF-based Virtual Nodules to Assess the Performance of Lung Cancer CT Screening CAD System. 12th Asia Oceania Congress of Medical Physics and 10th South East Asia Congress of Medical Physics, Chiang Mai Thailand, December 2012: 249-252.
4. **J.C. Marasinghe**, M. Ohkubo, H. Kobayashi, K. Murao,T. Matsumoto, S. Niizuma, S. Sone, S. Wada. Nodule Detection by Lung CT CAD: Analysis by PSF-based Image Simulation with Verification. Conference on Sri

Lanka Japan Collaborative Research, Peradeniya Sri Lanka, March 2013: 60.

5. S. Sivarajah, **J.C. Marasinghe**, M. Ohkubo, H. Kobayashi, M. Gohdo, S. Wada. Dependency of CT CAD Performance on the Distance Between Nodule and Pulmonary Vessel: A Study by Using Virtual Nodules. Conference on Sri Lanka Japan Collaborative Research, Peradeniya Sri Lanka, March 2013: 61.

6. Hajime Kobayashi, Masaki Ohkubo, **Marasinghe Janaka C**, Kohei Murao, Toru Matsumoto, Shusuke Sone, Shinichi Wada. A study of PSF-based virtual nodule for CAD performance evaluation of lung cancer CT screening. 106th Biannual Meeting of Japanese Society of Medical Physics, Osaka Japan, Japanese Journal of Medical Physics, Vol 33, Supplement No 3, September 2013: 81.

7. **J C Marasinghe**, M Ohkubo, H Kobayashi, K Murao,T Matsumoto, S Sone, S Wada. Evaluation of lung CT CAD performance by using PSF-based virtual nodules: a validation of the methodology. 20th Annual Conference on Medical Physics, Brighton, United Kingdom September 2013. Medical Physics International Journal, vol.1, No.2, 2013: 350.

8. Akifumi Yoshida, Masaki Ohkubo, Hajime Kobayashi, **J C Marasinghe**, D.M. Janaka Nuwan, Kohei Murao, Shuske Sone, Shinichi Wada. Influence in offset CAD performance evaluation of lung cancer CT screening. 107th Biannual Meeting of Japanese Society of Medical Physics,

Yokohama Japan, Japanese Journal of Medical Physics, Vol 35, Supplement No 1, April 2014: 127.

9. **J C Marasinghe**, M Ohkubo, H Kobayashi, A Yoshida, K Murao, T Matsumoto, S Sone, S Wada. Validation of using PSF-based virtual nodules to assess the basic performances of lung cancer CT screening CAD system. 28th International Congress and Exhibition of Computer Assisted Radiology and Surgery, Fukuoka, Japan. June 2014. International Journal of Computer Assisted Radiology and Surgery, (Suppl 1) 2014, 9: S236-S237.

10. Akifumi Yoshida, Masaki Ohkubo, **Marasinghe Janaka C**, Kohei Murao, Toru Matsumoto, Shinichi Wada. 胸部 CT 検診 CAD の QA に関する研究:ファントム模擬結節による virtual nodule offset の検証. 22nd Annual Meeting of Japanese Society of CT Screening, Osaka Japan 2015, Journal of Japanese Society of CT Screening, Vol. 22, No 1, February 2015: 36.

11. **J C Marasinghe**, M Ohkubo, H Kobayashi, A Yosida, K Murao, T Matsumoto, S Niizumz, S Sone, S Wada. Quality Assurance of lung cancer CT screening CAD system by applying PSF-based reference virtual nodule set. European Congress of Radiology 2015, Vienna, Austria March 2015.

Conference Presentations

1. **Janaka C Marasinghe**, Masaki Ohkubo, Hajime Kobayashi, Kohei Murao, Toru Matsumoto, Shinji Niizuma , Shusuke Sone, Shinichi Wada.

Performance assessment of CAD for lung cancer CT screening by applying PSF-based virtual nodules: Influence on slice thickness and nodule density. 104th Biannual Meeting of Japanese Society of Medical Physics, Tsukuba Japan, September 2012.

2. Hajime Kobayashi, Masaki Ohkubo, **Janaka C Marasinghe**, Kohei Murao, Toru Matsumoto, Shusuke Sone, Shinichi Wada. Performance assessment of CAD for lung cancer CT screening by applying PSF-based virtual nodules fusion onto screening CT images. 104th Biannual Meeting of Japanese Society of Medical Physics, Tsukuba Japan, September 2012.
3. **J C Marasinghe**, M Ohkubo, H Kobayashi, K Murao,T Matsumoto, S Niizuma , S Sone, S Wada. Application of PSF-based Virtual Nodules to Assess the Performance of Lung Cancer CT Screening CAD System. 12th Asia Oceania Congress of Medical Physics and 10th South East Asia Congress of Medical Physics, Chiang Mai Thailand, December 2012.
4. **J.C. Marasinghe**, M. Ohkubo, H. Kobayashi, K. Murao,T. Matsumoto, S. Niizuma, S. Sone, S. Wada. Nodule Detection by Lung CT CAD: Analysis by PSF-based Image Simulation with Verification. Conference on Sri Lanka Japan Collaborative Research, Peradeniya Sri Lanka, March 2013.
5. S. Sivarajah, **J.C. Marasinghe**, M. Ohkubo, H. Kobayashi, M. Gohdo, S. Wada. Dependency of CT CAD Performance on the Distance Between Nodule and Pulmonary Vessel: A Study by Using Virtual Nodules. Conference on Sri Lanka Japan Collaborative Research, Peradeniya Sri Lanka, March 2013.

6. Hajime Kobayashi, Masaki Ohkubo, **Marasinghe Janaka C**, Kohei Murao, Toru Matsumoto, Shusuke Sone, Shinichi Wada. A study of PSF-based virtual nodule for CAD performance evaluation of lung cancer CT screening. 106th Biannual Meeting of Japanese Society of Medical Physics, Osaka Japan, September 2013.

7. **J C Marasinghe**, M Ohkubo, H Kobayashi, K Murao,T Matsumoto, S Sone, S Wada. Evaluation of lung CT CAD performance by using PSF-based virtual nodules: a validation of the methodology. 20th Annual Conference on Medical Physics, Brighton, United Kingdom September 2013.

8. Akifumi Yoshida, Masaki Ohkubo, Hajime Kobayashi, **J C Marasinghe**, D.M. Janaka Nuwan, Kohei Murao, Shuske Sone, Shinichi Wada. Influence in offset CAD performance evaluation of lung cancer CT screening. 107th Biannual Meeting of Japanese Society of Medical Physics, Yokohama Japan, April 2014.

9. **J C Marasinghe**, M Ohkubo, H Kobayashi, A Yosida, K Murao, T Matsumoto, S Sone, S Wada. Validation of using PSF-based virtual nodules to assess the basic performances of lung cancer CT screening CAD system. 28th International Congress and Exhibition of Computer Assisted Radiology and Surgery, Fukuoka, Japan. June 2014.

10. Akifumi Yoshida, Masaki Ohkubo, **Marasinghe Janaka C**, Kohei Murao, Toru Matsumoto, Shinichi Wada. 胸部 CT 検診 CAD の QA に関する研究:ファントム模擬結節による virtual nodule offset の検証. 22nd

Annual Meeting of Japanese Society of CT Screening, Osaka Japan, February 2015.

Awards

- **Best oral presentation in medical imaging** at 12th Asia Oceania Congress of Medical Physics and 10th South East Asia Congress of Medical Physics, Chiang Mai Thailand, December 2012.
    - **J C Marasinghe**, M Ohkubo, H Kobayashi, K Murao,T Matsumoto, S Niizuma , S Sone, S Wada. Application of PSF-based Virtual Nodules to Assess the Performance of Lung Cancer CT Screening CAD System.

- Award for the **excellent research paper** by Japanese Society of Radiological Technology, North-East regional chapter.
    - Ohkubo M, Wada S, Kanai S, Ishikawa K, **Marasinghe JC**, Matsumoto T. Observer-independent nodule-detectability index for low-dose lung cancer screening CT: a pilot study. Radiol Phys Technol. 2013 Jul; 6(2):492-9. doi: 10.1007/s12194-013-0225-2. Epub 2013 Jun 9.